# In vitro coordination of Fe-protoheme with amyloid $\beta$ is non-specific and exhibits multiple equilibria

Jérôme Gout, Floriane Meuris, Alain Desbois, Pierre Dorlet

# *In vitro* Coordination of Fe-protoheme with amyloid β is non-specific and exhibits multiple equilibria

Jérôme Gout,[2] Floriane Meuris,[2] Alain Desbois*[2] and Pierre Dorlet*[1, 2]

[1]CNRS, Aix Marseille Université, BIP, IMM, Marseille, France

[2]Université Paris-Saclay, CEA, CNRS, Institute for Integrative Biology of the Cell (I2BC), Laboratoire Stress Oxydant et Détoxication, Gif-sur-Yvette, France

*To whom correspondence should be addressed : alain.desbois@netcourrier.com, pdorlet@imm.cnrs.fr

Keywords: amyloid β, heme, copper, Raman, EPR, metal-peptide interaction

**Abstract**

In addition to copper and zinc, heme is thought to play a role in Alzheimer's disease and its metabolism is strongly affected during the course of this disease. Amyloid β, the peptide associated with Alzheimer's disease, was shown to bind heme *in vitro* with potential catalytic activity linked to oxidative stress. To date, there is no direct determination of the structure of this complex. In this work, we studied the binding mode of heme to amyloid β in different conditions of pH and redox state by using isotopically labelled peptide in combination with advanced magnetic and vibrational spectroscopic methods. Our results show that the interaction between heme and amyloid β leads to a variety of species in equilibrium. The formation of these species seems to depend on many factors suggesting that the binding site is neither very strong nor highly specific. In addition, our data do not support the currently accepted model where a water molecule is bound to the ferric heme as sixth ligand. They also exclude structural models mimicking a peroxidatic site in the amyloid β-Fe-protoheme complexes.

## Introduction

Alzheimer's disease (AD) is a neurodegenerative disorder that causes the progressive and irreversible loss of brain functions including memory. This is the most common neurodegenerative disease. It is characterized by the appearance of senile plaques corresponding to aggregation of the amyloid beta (Aβ) peptide. The most prevalent forms of this peptide contain 40 (Aβ40) or 42 (Aβ42) aminoacid residues and consist of a largely hydrophilic N-terminal domain (first 16 residues Aβ16), and a C-terminal hydrophobic tail (17–40/42). The Aβ16 peptide contains all the ligands necessary for metal binding sites [1]. Indeed, in addition to aggregated Aβ peptides, the senile plaques include high concentrations of copper, zinc and iron [1]. In neurodegenerative diseases, the metabolism of these transition metals is largely affected and associated with oxidative stress phenomena [2]. Copper has been the metal most studied with respect to its interaction with the Aβ peptide due to its affinity in the $10^{10}$ $M^{-1}$ range [3]. At physiological pH, the Cu(II)-Aβ complex exists under two forms, so-called low-pH and high-pH forms, which are in equilibrium with each other with the low-pH form being predominant [4]. Both forms exhibit square-planar geometry. By contrast, Cu(I)-Aβ exhibits a digonal binding environment with two histidines as ligands [5].

In the past fifteen years, the interaction of heme with Aβ has also attracted attention. This followed reports that the deficiency of heme in brain cells led to decay reminiscent of what is observed in AD and indeed the metabolism of heme is altered in the brain of patients with AD [6, 7]. Some heme proteins such as hemoglobin or neuroglobin are overproduced in AD patients' brain and they co-localize with senile plaques [8, 9]. *In vitro*, heme can bind to the Aβ peptides [10-13] and the heme-Aβ complex has been shown to exhibit peroxidase activity [10, 11, 14, 15], to catalyze the oxidation of neurotransmitters such as serotonin [10, 16, 17], the nitration of tyrosines [15, 18, 19], and the reduction of nitrite [20]. There is no crystallographic structure of the heme-Aβ complex. Based on the peroxidase activity observed and spectroscopic studies with human and rodents Aβ [11] as well as mutants targeting the histidine residues [13], a structural model for heme binding to Aβ was proposed [11, 13]. According to this model, the ferric heme is coordinated in proximal position preferentially by His13 and a water molecule occupies the distal position. This water

molecule is hydrogen bonded to the Arg5 residue of the peptide [11, 13] that seems critical for peroxidase activity. This should be the resting state of the complex for its catalytic activity. However, an increasing ratio Aβ:heme was actually found to lead to better peroxidase activity [11]. As the increase of the Aβ concentration with respect to heme lead to the formation of low-spin complexes [6, 13], most likely bis-His coordinated, this is somewhat counterintuitive. In addition, some studies have questioned the biological relevance, active site structure and the specificity of heme-Aβ peroxidase activity towards external substrates [15, 21-24]. It should also be noted that if mutations can help the ligands determination of metal site, it remains an indirect way since they can induce structural rearrangements that could also explain the experimental observations.

In this work, we have used advanced techniques such as pulse electron paramagnetic resonance (EPR) and resonance Raman (RR) spectroscopies in combination with specific isotopic labelling of the Aβ16 peptide to better probe its interaction with heme. We have also studied this interaction in presence of copper since its coordination to Aβ is well characterized and therefore enabled us to use it as a probe. Our results show that the interaction between heme and Aβ leads to a variety of species with different coordination states. In particular, we could exclude the presence of a water molecule as a sixth ligand in the ferric state for the high-spin species. We also exclude the formation of a peroxidase-like site in the Aβ-heme complexes. The formation of these species seems to depend on many factors suggesting that the binding site is relatively weak and unspecific. In the presence of copper, we did not detect a preferential binding site for heme as its presence did not affect the coordination of Cu(II) for the predominant species at physiological pH.

## Materials and Methods

**Materials.** Unlabeled human Aβ16 peptide (DAEFRHDSGYEVHHQK) and Aβ40 peptide (DAEFRHDSGYEVHHQKLVFFAEDVGSNKGAIIGLMVGGVV) were purchased from GeneCust (Dudelange, Luxembourg). Labeled histidine (L-histidine-N-fmoc, $^{15}N$, 98%) was bought from Eurisotop (Saclay, France). Aβ16 peptides including one labeled histidine at position 6, 13 or 14 were synthesized by GenePep (Prades-le-Lez, France). Peptide concentrations in solution were determined by UV–visible absorption spectroscopy. Human Aβ40 peptide was

prepared by freshly dissolving the powder in 0.1 M NaOH (pH≈13) to give a stock solution of 1 to 5 mM. The treatment with NaOH was done to minimize oligomerization of the peptide [25] and the stock solution was subsequently diluted for sample preparation. All samples were visually checked for precipitation. In this line, the Raman investigations did not show any anomalously wide Rayleigh band that could be indicative of large diffusions of the samples. In the case of EPR, samples were freshly prepared and immediately frozen in liquid nitrogen preventing any evolution of the sample. Chemicals were purchased from Sigma. Different buffers were used at different pH ranges: 3-(N-Morpholino)propanesulfonic acid (MOPS) for pH 6.7 and N-Cyclohexyl-2-aminoethanesulfonic acid (CHES) for pH 9. Hemin solution was freshly prepared by dissolving the powder in 0.1 M NaOH. A solution of 0.1 M sodium monophosphate was added to adjust the pH value at 7.5.

**Electronic absorption spectroscopy.** UV-visible spectra were measured using a Uvikon XL spectrophotometer (Sekoman).

**Electron paramagnetic resonance spectroscopy.** Continuous-wave EPR spectra were recorded using a Bruker Elexsys E500 spectrometer equipped with a continuous flow cryostat (Oxford). Pulse EPR experiments were performed with a Bruker Elexsys E580 spectrometer at liquid helium temperatures. 4-pulse hyperfine sublevel correlation (HYSCORE) spectra were recorded with the usual four-pulse sequence $\pi/2$-$\tau$-$\pi/2$-$t_1$-$\pi$-$t_2$-$\pi/2$ with a length of 24 ns for all pulses and the power of the $\pi$ pulse was adjusted accordingly. The size of the data was 256x256, the time intervals $t_1$ and $t_2$ were varied from 88 to 4168 ns in steps of 16 ns. The $\tau$ value was fixed (136 ns). A four-step phase cycle was used to eliminate unwanted echoes. The time domain spectra were baseline corrected, apodized with a Hamming window and zero-filled. Pulse EPR data were processed by using routines locally written with Matlab (The Mathworks, Inc.).

**Resonance Raman spectroscopy.** RR spectra were recorded using a Jobin-Yvon spectrometer (either U1000 or T64000 model), equipped with a liquid nitrogen cooled charge-coupled device detector (Spectrum One, Jobin-Yvon). The ferric samples were excited in the Soret region with the 363.8 nm line of an Ar laser (Coherent Innova), the 413.1 nm line of a $Kr^+$

laser (Coherent Innova) and the 441.6 nm line of a He/Cd laser (Liconix). The ferrous forms were investigated with the 413.1- and 441.6-nm excitations. Low laser powers (5-15 mW), neutral filters and/or defocalisation of the laser beams were used to minimize either the photoreduction of the ferric samples or the photodissociation of the ferrous CO compounds. The signal-to-noise ratios were improved by spectral collections of 6-8 cycles of 30 seconds accumulations time. The reported spectra were the results of averaging 5-6 single spectra. The spectral analysis was made using the Grams 32 sofware (Galactic Industries). The frequency precision was 0.5-1 $cm^{-1}$ for the most intense bands and 1.5-2 $cm^{-1}$ for the weakest bands.

**Results**

At physiological pH (7.4), the binding of Cu(II) to Aβ yields a mixture of two complexes, a low pH form and a high pH form, in equilibrium [26]. Each of these complexes is largely predominant at pH 6.7 and 9.0, respectively. In order to separate contributions and better study the impact of copper binding on the heme-Aβ interactions, our experiments were mainly performed at these two pH values.

**Electronic absorption spectroscopy.** At pH 6.7, mixing Fe(III)-protoheme IX (Fe(III)PP) with Aβ peptide at a molar ratio of 1:1 induced a redshift and an intensity increase of the Soret band above 400 nm (see Figure 1, left panels). This indicates that the ferriheme binds to the peptide. The shape of the bands suggests a mixture of species with the formation of a minor low-spin (LS) species. The contribution of the LS complex is higher for the Aβ40 peptide than for the Aβ16 compound. The results are similar to previous observations at physiological pH [11, 13]. The addition of one equivalent (eq) of Cu(II) ions to the heme-Aβ mixture at this pH provokes the removal of the LS contribution and yields a broad spectrum compatible with heme bound to the peptide in a high-spin (HS) complex. Mixture with free hemin cannot be excluded. At pH 9, the changes observed by the addition of hemin and Cu(II) are much less drastic (Figure 1, right panels). The shape of the spectrum is not affected, there is only a small increase in intensity. The only significant change is observed for the heme-Aβ40 complex (broadening of the spectrum and decrease in absorbance) and is reversed by the

addition of 1 eq of Cu(II) ions. Based on these spectra, it is not possible to conclude about a specific interaction between heme and Aβ peptide at this pH. Further investigations are needed with other spectroscopies.

**EPR spectroscopy.** To further examine the interaction between ferriheme and Aβ peptide, we collected X-band EPR data on the complex in the presence or absence of Cu(II) ions. At pH 6.7, the hemin sample exhibits its axial high-spin (HS) signal characteristic of the S=5/2 state. In presence of the Aβ peptide, the HS signal is not modified (see also Figure S1). It is therefore difficult to conclude whether it still corresponds to free hemin or to a HS complex between heme and the peptide. By contrast, a low-spin (LS) ferric heme signal is observed in the high-field region with g-values of 2.95 and 2.26 (the third g-value is not clearly detected which is usual for this type of species), indicating an interaction between heme and the Aβ16 or Aβ40 peptide. The LS signal is saturated under the recording conditions used here for the HS signal but it is clearly visible nonetheless. Upon addition of 1 eq of Cu(II), the heme-peptide LS signal disappears and only the HS signal is observed for the ferric heme. In the g=2 region, the EPR spectrum of the complex between Cu(II) and Aβ peptide is observed and is identical to that observed in the absence of hemin ($A_{//} \sim$ 540MHz, $g_{//} \sim$2.26, and $g_{\perp} \sim$2.06) [27-29].

At pH 9.0, the hemin sample exhibits a more complex HS signal due to the alkaline conditions. This EPR spectrum is not modified by the addition of 1 eq of Aβ peptide and no LS signal is observed contrarily to what is detected at pH 6.7. This suggests that either i) there is no interaction between the heme and the Aβ peptides, or ii) this interaction is not specific enough to significantly modify the EPR properties of the HS species formed. The addition of 1 eq of Cu(II) yields the corresponding EPR spectrum of the Cu(II)-Aβ complex at this pH in the g=2 region. Once again, the presence of hemin does not affect the EPR properties of the Cu(II)-Aβ complex at pH 9.0 ($A_{//} \sim$ 495 MHz, $g_{//} \sim$2.23, and $g_{\perp} \sim$ 2.06) [27]. In addition, the low field spectrum corresponding to the HS heme moiety is also not affected by the presence of Cu(II).

In order to better probe the reciprocal influences of the interactions between Aβ peptide, ferriheme and Cu(II), we performed pulse EPR experiments to specifically address the binding of histidine (His) residues from the peptide to Cu(II) and heme. For this purpose, we

used Aβ16 peptides specifically labelled with $^{15}N$ on either His6, His13 or His14 as was done previously to determine the coordination sphere of Cu(II) in the Aβ peptide [27]. Due to the relaxation properties of the HS ferric species, we could not obtain data from HYSCORE measurements on our setup to directly study the interaction between heme and the Aβ16 peptide. Therefore, we could not probe whether there was a preferential binding of one of the His as has been proposed in the literature [13]. However, we could probe the coordination sphere of the Cu(II) ion and check whether the presence of heme had any effect on its binding with the available His residues. The use of a labelled peptide is a better approach than that using mutants, because modifying aminoacids in the sequence could have effects on the structural properties of the peptide as well as on the binding properties towards metal ions.

The HYSCORE contour plots obtained on Aβ16 peptide mixed with 1 eq of ferric heme and 1 eq of Cu(II) ions are presented in Figure 3. The characteristic cross-peaks at [(4; 1.5),(1.5; 4)] MHz arise from the remote $^{14}N$ nucleus (nuclear spin I=1) from the His imidazole ring coordinated to the Cu(II) ion in equatorial position [27]. When labelled with $^{15}N$ (I=1/2), the corresponding cross-peaks appear at [(0.3; 2.6),(2.6; 0.3)] MHz. These peaks are visible for each labelled His residue (His6, His13 or His14) indicating they all participate in Cu(II) coordination. At pH 6.7, the cross-peaks for labelled His6 are more intense compared to His13/His14 which is similar to what was observed for the Cu(II)-Aβ16 complex [27]. The presence of heme does not affect the coordination of the Cu(II) ion. At pH 9.0, the cross-peaks for labelled His6 are also more pronounced compared to His13/His14. This differs slightly from the Cu(II)-Aβ16 complex for which all signals were roughly equivalent. Therefore, at this pH, the presence of heme has some influence on which His residue coordinates the Cu(II) ion.

**RR Spectroscopy.** ***Fe(III)-protoheme complexes.*** The broad absorption spectra of the Aβ-ferriprotoheme (Aβ-Fe(III)PP) complexes suggest a mixing of various species (see above, Fig. 1 and [10, 11, 13, 15, 30]). In order to characterize these forms, we used RR spectroscopy with three Soret excitations (363.8, 413.1 and 441.6 nm). For the Aβ16- and Aβ40-Fe(III)PP complexes formed with a stoichiometry of 1 eq of peptide/heme at pH 6.7, the high-frequency RR spectra (1300-1650 $cm^{-1}$) excited with the 413.1 and 441.6 nm lines exhibit a

pair of bands of variable intensity in the $\nu_{10}$, $\nu_2$ and $\nu_3$ regions (1626/1640, 1570/1580 and 1490/1505 $cm^{-1}$, respectively) (Figure 4 spectrum(a), Figure S2 and spectra not shown). The 363.8 nm-excited spectrum mainly shows the 1626, 1570 and 1490 $cm^{-1}$ components (Figure S2). The v3 regions (1480-1510 cm-1) clearly show that the LS contribution is mostly RR-active with the 413.1-nm excitation (Figure S2). Table 1 lists the frequencies of the observed main modes of the Aβ40- and Aβ16-Fe(III)PP complexes at pH 6.7. The RR spectra of the Aβ16-Fe(III)PP complexes prepared under the same experimental conditions (1 eq Aβ16/heme, pH 6.7) are highly similar in terms of band frequencies (Figure S3; Table 1). However, the major spectral contribution concerns the LS form for Aβ40 while the contrary occurs for Aβ16 (Figure S3, spectra (a) and (c)). All these observations establish the co-existence of five-coordinated (5c) HS and six-coordinated (6c) LS forms [31-33]. When the concentration of the Aβ40 or Aβ16 peptide is increased at 2 eq/heme, the spectral contributions of the 6cLS form are increased (spectra not shown). This is in line with what was observed by UV-visible spectroscopy [11]. Changes in pH values from 6.7 to 9.0 increase the relative intensities of the skeletal modes of the 5cHS species. This effect is particularly marked for the Aβ40 peptide (Figure S3). Addition of 1 eq of Cu(II) ions to the Aβ-Fe(III)PP complex preformed at pH 6.7 or 9.0 apparently abolishes the contributions of the RR bands arising from the 6cLS species in the 441.6-nm excited spectra (see Figure S4 for the Aβ16 peptide). However, the 413.1-nm excited spectra show the conservation of minor contributions of this 6cLS species (Figures S5 and S6). It is important to note that in the course of the various performed titrations (peptide/heme ratio, pH change, and Cu(II) addition), we observe different enhancement patterns of the 5cHS and 6cLS species but no contribution of any 6cHS form for which RR bands are expected at 1480-1483 ($\nu_3$), 1559-1563 ($\nu_2$) and 1608-1610 ($\nu_{10}$) $cm^{-1}$ [31-33].

***Fe(II)-protoheme complexes.*** The high-frequency RR spectra of the Aβ40-Fe(II)PP complexes also indicate a mixture of two species (Figure 4 spectrum (b), Table 1). On the one hand, bands observed at 1357 ($\nu_4$), 1469 ($\nu_3$), 1545 ($\nu_{11}$), 1561 ($\nu_2$), and 1602 ($\nu_{10}$) $cm^{-1}$ are characteristics of a 5cHS form [31-33]. On the other hand, a 6cLS complex is present as judged by the spectral contributions detected at 1366 ($\nu_4$), 1496 ($\nu_3$), 1532 ($\nu_{11}$), 1580 ($\nu_2$), and 1617 ($\nu_{10}$) $cm^{-1}$ (Figure 4 spectrum (b)) and spectra not shown, Table 1) [31-33].

A mode involving major stretching of the axial Fe-N(His) bond of His-coordinated 5cHS ferrous hemoproteins is observed in the 200-260 $cm^{-1}$ region and is RR-enhanced with the 441.6-nm excitation [34-43]. In the low-frequency RR spectrum of the Aβ40-Fe(II)PP complexes excited at this wavelength, we observed a specific line at 221 $cm^{-1}$ (Figure 5 (spectrum (a)). This band is absent in the 413.1 nm-excited spectrum (spectrum not shown). We thus assign this 221 $cm^{-1}$ band to the ν(Fe-His) mode of the 5cHS species of the Aβ40-Fe(II)PP complexes. A band observed at 238 $cm^{-1}$ could be assigned to a ν(Fe-His) mode of a minor 5cHS component (Figure 5, spectrum (a)). The RR spectrum excited at 413.1 nm however presents a similar 240 $cm^{-1}$ feature accompanied by bands of the 6cLS species at 348, 381 and 417 $cm^{-1}$ (Table 1). If one consider that the 238-240 $cm^{-1}$ features are RR-active at both 413.1 and 441.6 nm, these bands are rather assigned to the $\nu_{52}$ mode observed at 235-242 $cm^{-1}$ in the RR spectra of various 6cLS compounds [44-47].

***Carbonyl Fe(II)-protoheme complexes (Aβ-Fe(II)PPCO).*** The high-frequency RR spectra of the Aβ40-Fe(II)PPCO species excited at 441.6 and 413.1 nm show skeletal modes at 1372 ($\nu_4$), 1501 ($\nu_3$), 1583 ($\nu_2$) and 1630 ($\nu_{10}$) $cm^{-1}$ (Figure 4, spectrum (c) and spectra not shown). These frequencies are typical of CO-bound ferrous complexes [32]. The weak features observed at 1357, 1469 and 1603 $cm^{-1}$ represent a 5cHS photodissociated form (Figure 4), the intensities of these bands increase when the photolysis level is increased. The high-frequency RR spectra of the Aβ16-Fe(II)PPCO complexes are very similar to those of the Aβ40-Fe(II)PPCO species, both in terms of band intensities and band frequencies (Spectra not shown, Table 1).

The Fe-CO stretching (ν(Fe-CO)) modes of the hemoproteins and model compounds were observed in the 460-550 $cm^{-1}$ region of RR spectra [48-52]. The low-frequency RR spectra of the Aβ40-Fe(II)PPCO species excited at either 413.1 or 441.6 nm are presented in Figure 5. In these spectra, two bands are assignable to ν(Fe-CO) modes. The 441.6 nm-excitation indeed enhances a ligand-specific band at 496 $cm^{-1}$ while the 413.1 nm-excitation activates not only this band but also a 526 $cm^{-1}$ band. An increase in peptide concentration at 2 eq/heme increases the relative contribution of the 526 $cm^{-1}$ line by *ca.* 30 % when the spectra are normalized on the intensities of the bands at 677 $cm^{-1}$ ($\nu_7$) and 349 $cm^{-1}$ ($\nu_8$) (spectra not shown). Therefore, the 526 $cm^{-1}$ band cannot be assigned to a ν(Fe-CO) mode originating from a free Fe(II)PP-CO complex. The low-frequency RR spectra of the Aβ16-Fe(II)PPCO

complexes exhibit close features with ν(Fe-CO) modes at 496 and 529 $cm^{-1}$ (spectra not shown, Table 1). However, the relative contributions of the 529 $cm^{-1}$ component of Aβ16-Fe(II)PPCO are increased twofold when compared to those of the 526 $cm^{-1}$ component of Aβ40-Fe(II)PPCO. This indicates that the minor B form has a more important relative population in the Aβ16-Fe(II)PPCO complexes.

The 441.6- and 413.1-nm excitations of the Aβ-Fe(II)PPCO complexes enhance the CO stretching (ν(CO)) modes (Figure 6, Table 1). In the 1920-2000 $cm^{-1}$ regions of the RR spectra of Aβ40-Fe(II)PPCO at pH 7.4, we observe two overlapping bands at 1957 and 1964 $cm^{-1}$. The 1964 $cm^{-1}$ line is mostly enhanced with the 441.6-nm excitation while the 1957 $cm^{-1}$ line is mainly RR-activated with the 413.1-nm laser line (Figure 6). The RR spectra of the Aβ16-Fe(II)PPCO complexes at pH 7.4 exhibit similar features with ν(CO) modes at 1956 and 1963 $cm^{-1}$ (Table 1). Changes in pH value (6.7 or 9.0) and/or presence of Cu(I) ion (1eq/heme) to the Aβ16-Fe(II)PPCO complexes produce small changes in relative intensity and frequency of the ν(Fe-CO) and ν(CO) bands (spectra not shown, Table S1).

***Peripheral Aβ-heme interactions.*** The RR spectra of heme proteins include a number of modes involving the tetrapyrrole substituents. These modes allow the investigations of the peripheral heme-protein interactions [32, 53]. Table 1 lists the frequencies of the most intense bands involving the vinyl, methyl and/or propionate groups of FePP. In particular, we observed a single band at 1620-1621 $cm^{-1}$ for the ν($C_a$=$C_b$) vinyl mode (Figure 4, Table 1). Significant frequency differences concern the δ($C_\beta$(pyrrole)-$C_aC_b$ (vinyl)) and δ($C_\beta$(pyrrole)-$C_aC_b$(propionate)) modes of the 5cHS species when compared to those of the 6cLS species (411-413/417-419 and 377-378/381-383 $cm^{-1}$, respectively) (Table 1).

## Discussion

**Ferric forms.** UV-visible absorption data indicates a mixture of HS and LS species when ferric heme is mixed with Aβ peptide at pH 6.7. The LS species is not predominant at equimolar concentration. This is also supported by EPR data which exhibit a LS signal whose g-values are in agreement with a bis(His) ligation for the heme. The amount of LS species increases with the peptide/heme ratio (not shown and [11]). Therefore, it can be attributed to a complex in which two Aβ peptides coordinate the heme by one His residue each. This also

implies that there is an equilibrium with free hemin in the sample. There must also be a 5cHS complex between heme and one peptide providing a His ligand. However, in this case the HS EPR signal of the complex and of free hemin cannot be distinguished but further information is obtained by RR spectroscopy (see below). What is clear is that the formation of the LS signal is inhibited by the addition of 1 eq of Cu(II). HYSCORE experiments performed on the Cu(II)-Aβ16-heme complex labelled with $^{15}N$ on either histidine residues yields results quite similar to what was obtained in the study of the Cu(II)-Aβ16 complex [27]. The affinity of Cu(II) for the Aβ peptides is at least 3 orders of magnitude higher than that of Fe(III)PP [3, 54, 55]. Cu(II) forms a 1/1 complex with the Aβ peptide but its intramolecular coordination is heterogeneous, depending on pH [3, 4, 29, 54-59]. At pH 6.7, Cu(II) is coordinated in a square planar geometry by four ligands among which His6 on one position and His13 or His14 on another while at pH 9.0 only one His (either His6, His13 or His14) participates to the coordination sphere [4, 27]. In the presence of heme, the spectra at pH 6.7 are unaffected. Since only two His residues are involved in Cu(II) coordination, this leaves one free to bind heme. However, there is apparently no preferential binding of His13 or His14 to heme since both equally participates in the coordination of Cu(II). On the contrary, the coordination of His6 to Cu(II) at pH 9.0 seems to be favored in the presence of heme thus leaving a preferential binding of His13 or His14 to the heme. The latter His residues are detected as Cu(II) ligands and therefore the coordination of heme is expected to be a mixture in equilibrium of the 5cHS Fe(III)PP-His13(Aβ) and Fe(III)PP-His14(Aβ) forms.

In the RR spectra, the behavior of the spin-state markers bands $\nu_2$, $\nu_3$ and $\nu_{10}$ of the Aβ-Fe(III)PP complexes as a function of the heme-peptide stoichiometry provide evidence for the formation of 5cHS and 6cLS species, the latter species being stabilized when the peptide/heme molar ratio is increased. The 5cHS species exhibits the $\nu_3$, $\nu_2$ and $\nu_{10}$ modes at 1490, 1570 and 1626 $cm^{-1}$, respectively, and shows no marked pH-dependence. This observation suggests the absence of $H_2O$ or $HO^-$ binding in 6$^{th}$ coordination position. The 5cHS frequencies of the Aβ16- and Aβ40-Fe(III)PP complexes fall close to those determined for 5cHS Fe(III)PP complexes with a neutral imidazole ring (1490-1494, 1563-1569 and 1624-1628 $cm^{-1}$) [60, 61]. When the fifth axial ligand has an imidazolate character, the strong σ-bonding interaction of this anionic ligand with the Fe(III) ion induces frequency upshifts (1494-1500, 1570-1575 and 1629-1631 $cm^{-1}$, respectively) [62, 63]. Therefore, the 5cHS

species can be described as an equimolar Aβ-ferriheme complex in which the 5th axial ligand of heme is a neutral imidazole from a His residue, most likely His13 or His14 (Fe(III)PP-His13(Aβ) and/or Fe(III)PP-His14(Aβ)) [11, 13, 21, 64, 65]. Structural models in which the HS species of the Aβ-ferriheme complexes is 6c with a water molecule as a sixth ligand are thus irrelevant [15, 64]. In the frame of a 1/1 Aβ-heme complex, the formation of a 5cHS species could result from a polypeptide fold that could not provide a distal aminoacid able to stabilize a bound $H_2O$ via H-bonding. Given the number of polar side chains and the flexibility of the hydrophilic 1-16 fragment of the Aβ peptides, this scenario seems unlikely, in particular for the short Aβ16 compound. It is however well known that the Aβ peptides and Fe(III)PP in aqueous solutions exist in various levels of aggregation [45, 66, 67]. A 2/2 Aβ-heme 5cHS complex could be therefore built from a π-stacking of two hemes included in a cleft formed by two Aβ peptides (Aβ-[Fe(III)PP]$_2$-Aβ). Upon increase in relative Aβ concentration at a 2/1 Aβ/heme ratio, the heme π-dimer could be dissociated and each heme monomer could bind a second Aβ molecule according to the following reaction :

$$(\text{Aβ-[Fe(III)PP]}_2\text{-Aβ})_{(5cHS)} + 2\ \text{Aβ} \rightarrow 2\ (\text{Aβ-Fe(III)PP-Aβ})_{(6c\ LS)}$$

The 6cLS species exhibits the skeletal $\nu_3$, $\nu_2$ and $\nu_{10}$ modes at 1505, 1580 and 1640 $cm^{-1}$, respectively (Table 1). These frequencies are very close to those of Fe(III)PP complexed with two neutral imidazole rings (1505, 1579 and 1641 $cm^{-1}$) [45]. The RR spectra of the 6cLS species are in agreement with a heme coordination via the His side chain of two Aβ units. Our RR spectra also showed that the Cu(II) ion inhibited the formation of the 6cLS species but did not affect that of the 5cHS species. Considering that His6 is the most involved His residue in the Cu(II) sites, the bis(His6) as well as the mixed His6/His13 and His6/His14 ligations of Fe(III)PP are not allowed when the Cu(II) ion is bound to the Aβ peptides. The minor contributions of 6cLS bands in the RR spectra of the Aβ-Fe(III)PP-Cu(II) complexes indicate a limited formation of bis(His13), bis(His14) and mixed His13/His14 coordinations. This is too low to be detected in the EPR experiments. A particular conformation of the Aβ-Cu(II) peptides apparently prevents an appropriate presentation of two axial histidylimidazole side chains for Fe(III)PP insertion.

**Ferrous forms.** The high-frequency RR spectra of the Aβ40-Fe(II)PP complexes clearly established the formation of 5cHS and 6cLS species (Table 1) [31-33]. By analogy with

previous studies on deoxyhemoproteins and model compounds [38-40, 42], the specific 221-225 $cm^{-1}$ band seen in the 441.6-nm excited RR spectra of Aβ40-FePP and of the photodissociated state of the Aβ40-FePPCO and Aβ16-FePPCO complexes can be assigned to a ν(Fe-His) mode of the 5cHS species of the Aβ-ferroheme complexes (Table 1). Deoxymyoglobins which have a weak H-bond on the axial His ligand show a ν(Fe-N(His)) at 220-224 $cm^{-1}$ [39, 53]. In the 5cHS Aβ- Fe(II)PP complexes, the link between Fe(II)PP and peptide is thus constituted by a neutral axial imidazole ligand weakly H-bonded to its protein environment.

In the RR spectra of a reduced Aβ-FePP complex, Gosh et al. [64] observed a band at 241 $cm^{-1}$ and assigned it to a Fe-His stretching mode. However, this investigation used a 413.1 nm excitation that is not favorable for the observation of such an axial mode of a Fe(II)-protoheme. Indeed, the ν(Fe-His) mode is coupled to imidazole and porphyrin deformation modes and draws its RR activity from the planar π-π* Soret transition [34-37, 41, 43]. Excitation profiles of deoxymyoglobin showed that the intensity of the mode involving the axial Fe-His bond follows the shape of the Soret absorption band that peaks at 434 nm [35, 36]. For reduced peroxidases, the anionic character of the axial His results in high ν(Fe-His) frequencies (243-255 $cm^{-1}$) and redshifts of the Soret maximum at 437-446 nm [42, 53, 62, 68-71]. A 413.1 nm-excitation is clearly unappropriate for the observation of a ν(Fe-N(Histidinate)) mode [72, 73].

As far as the 6cLS ferrous form is concerned, we did not detect any stretching mode involving the axial ligands. However, the $\nu_{11}$ mode of the 6cLS bis(imidazole) complexes of ferrohemes is a π-electron marker band sensitive to the donor strength of the axial ligands [45]. For the corresponding species of Aβ-Fe(II)PP, we observed this mode at 1532 $cm^{-1}$ (Table 1). This frequency is very close to that determined for Fe(II)PP coordinated by two neutral imidazole rings (1533 $cm^{-1}$) [45].

The frequencies of the modes involving stretching of the vinyl heme groups indicate equivalent and unstrained conformations for the 2- and 4- vinyl substituents (Table 1). The frequency differences observed for the $C_\beta$(pyrrole)-$C_aC_b$(vinyl) and $C_\beta$(pyrrole)-$C_cC_d$(propionate) deformation modes of the ferric and ferrous 5cHS species when compared to the ferric and ferrous 6c LS species are likely due the 5c state that induces a porphyrin

doming and thus changes in steric and/or electrostatic interactions between the peripheral protoheme substituents and the Aβ polypeptides.

**Ferrous CO forms.** Carbon monoxide is a ligand that provides information about the ligand-ferroheme environment in heme proteins [48-52]. The RR spectra of the Aβ40-Fe(II)PPCO and Aβ16-Fe(II)PPCO showed two sets of ν(Fe-CO) and ν(CO) modes. On the basis of the variations in band intensity as a function of the exciting wavelength, the ν(Fe-CO) bands at 495-498 $cm^{-1}$ are associated to the ν(CO) components at 1961-1964 $cm^{-1}$ (A form) while the ν(Fe-CO) bands at 526-532 $cm^{-1}$ are related to the ν(CO) bands at 1953-1957 $cm^{-1}$ (B form) (Table 1, Table S1). It is well established that the ν(Fe-CO) and ν(CO) frequencies of heme proteins and their model compounds display inverse linear correlations. This effect is due to a back-donation of Fe(II) $d_\pi$ electrons to the CO $\pi^*$ orbitals [48-52]. For ligand-Fe(II)PPCO systems, these linear correlations primarily depend on the nature and electronegativity of the ligand trans to the CO grouping (Figure 7) [48-51, 72, 74-91]. The sets of frequencies of the major A component (495-498/1961-1964 $cm^{-1}$) fall on the correlation line of heme-CO complexes with a neutral histidine or neutral imidazole as a $5^{th}$ ligand (Figure 7). Moreover, the position of a given point on a correlation line reflects the polarity of the CO environment. Positive dipoles or H-bonds generate high ν(Fe-CO) and low ν(CO) frequencies. In these cases, the points are located toward the left end of the correlation line. Negative dipoles do the opposite and locate the ν(Fe-CO)/ν(CO) frequencies on the right side of the correlation line. The points corresponding to the A form of the Aβ40- and Aβ16- Fe(II)PPCO complexes (495-498/1961-1964 $cm^{-1}$) indicate a distal environment that is essentially hydrophobic (Figure 7). Carbonyl ferromyoglobins for which a distal His residue forms a weak H-bond with the bound CO exhibit ν(Fe-CO) and ν(CO) modes at 507-512 and 1941-1947 $cm^{-1}$, respectively [85, 91]. When this distal His is replaced by a hydrophobic residue (His → Gly, Leu, or Ile), the ν(Fe-CO)/ν(CO) frequencies are observed at 490-492/1965-1968 $cm^{-1}$ and approach those of the A form of the Aβ-Fe(II)PPCO complexes [84, 87, 90]. The CO ferrous derivatives of *Glycera dibranchiata* hemoglobin and of the oxygen-sensor Fix L exhibit ν(Fe-CO)/ν(CO) modes at 496/1967 $cm^{-1}$ and 498/1962 $cm^{-1}$, respectively [83, 89]. The crystal structures of these proteins confirm this trend since they indicate a hydrophobic distal part of the heme pocket and a lack of a residue able to form a H-bond with a 6th ligand [92, 93].

All these comparisons allow us to conclude that the heme of the major A form of the Aβ40- and Aβ16- Fe(II)PPCO complexes is coordinated, on the one hand, by a neutral His and, on the other hand, by a CO ligand immersed in a hydrophobic environment unable to make a H-bond. The weak peroxidase activity of the Aβ-FePP complexes was reported to be supported by a heme coordination by a proximal histidinate-like ligand and the proximity of a distal arginine residue interacting with the sixth ligand [65]. Such a model cannot be retained on the basis of the present RR data. The observation of a neutral His ligand in the major A form of the Aβ-Fe(II)PPCO complexes is consistent with the detection of a ν(Fe-His) mode at 221-225 $cm^{-1}$ for the 5cHS ferrous form as well as the $\nu_{11}$ mode at 1532 $cm^{-1}$ for the 6c LS ferrous form.

The second series of ν(Fe-CO)/ν(CO) frequencies at 526-532 and 1953-1957 $cm^{-1}$ (B form) is located on a correlation line corresponding to a neutral oxygenated 5$^{th}$ ligand (Figure 7). The best RR activity of these modes with the 413.1 nm excitation is associated with a blue shifted Soret band when a weak ligand replaces a neutral imidazole ring [78, 81]. The ν(Fe-CO)/ν(CO) frequencies of the B form are close to those recorded for the H23G mutant of myoglobin (522/1960 $cm^{-1}$) and the H25Y mutant of heme oxygenase-1 (529/1962 $cm^{-1}$) in which the proximal His ligand of heme is replaced by either a water molecule or a hydroxyl group of a Tyr residue [74, 78, 88]. The positions on the medium part of the correlation line are indicative of a H-bonded CO ligand like that observed for the H23G mutant of myoglobin which retains a distal histidine (His64). The spectral contribution of the B form is increased when the Aβ/heme ratio is increased from 1/1 to 2/1. These observations suggest that the Fe(II)PPCO moiety of the B form is accomodated by two peptides units, one Aβ providing the proximal O-ligand and the second Aβ molecule stabilizing the bound CO via an H-bond donor. The side chain of Tyr10 or a water molecule could be a good candidate for the axial O-ligation. Further studies are required to fully characterize the B form of the Aβ-Fe(II)PPCO complexes.

The binding of Cu(I) ion to the Aβ16-FePPCO complexes did not strongly affect the intensities and frequencies of ν(Fe-CO) and ν(CO) modes (Table S1). Cu(I) has a very high affinity for Aβ16 and coordinates to the peptide under a linear geometry through two of the three available histidine residues [5, 94, 95]. Our RR data show that the bis(His) coordination of

Cu(I) has no major influence on the formation and structure of the A and B forms of the Aβ16-Fe(II)PPCO complexes.

## Conclusion

This work demonstrates that the Aβ-heme complexes adopt various structures, depending on the Aβ/heme stoichiometry, the oxidation state of the FePP as well as the presence and the nature of a sixth heme ligand. Overall, the nature of the peptide (Aβ16 or Aβ40) did not have a strong effect on the results, supporting the fact that the Aβ40 peptide was mostly monomeric in the experiments. The equilibria of these structures are in addition dependent on the pH value and the presence of Cu. The absence of well-defined structures in the Aβ-heme complexes suggests weak and/or strained peptide-Fe(III/II)PP interactions. In this line, when the Aβ/hemin ratio is equal to 1, no water molecule is bound to the Aβ-Fe(III)PP complexes. For the ferrous CO complexes, no folding of the Aβ peptides permits both the coordination of a proximal His residue and an H-bonded CO ligand. These two examples illustrate the difficulties of structuration of the Aβ peptides around the heme. Finally, the coordination of the iron center by a His residue close to an arginine or a tyrosine residue has motivated the proposal of an active site in Aβ-heme complexes similar to that characterized in heme peroxidases. Our spectroscopic results exclude such a structural scheme in the Aβ-heme complexes. Due to the influence of many factors on the Aβ-heme complex formation and state, as well as contradictory results from the literature on *in vitro* studies, it is likely that an increase in *in vivo* studies [96] will lead to better biologically relevant conclusions.

## CRediT author statement

**Jérôme Gout**: Investigation. **Floriane Meuris**: Investigation. **Alain Desbois**: Investigation, Methodology, Validation, Visualization, Writing- Reviewing and Editing. **Pierre Dorlet**: Conceptualization, Investigation, Methodology, Validation, Visualization, Writing- Reviewing and Editing, Funding acquisition.

## Acknowledgments.

Funding from the Agence Nationale de la Recherche (Programme Blanc NT09-488591, “NEUROMETALS”) is acknowledged. We thank Jérôme Santolini for help in preliminary

resonance Raman data acquisition and discussions, and Christelle Hureau and Peter Faller for fruitful discussions.

## References

[1] C. Hureau, Coordination of redox active metal ions to the amyloid precursor protein and to amyloid-β peptides involved in Alzheimer disease. Part 1: An overview, Coord. Chem. Rev. 256 (2012) 2164-2174. https://doi.org/https://doi.org/10.1016/j.ccr.2012.03.037.
[2] C. Cheignon, M. Tomas, D. Bonnefont-Rousselot, P. Faller, C. Hureau, F. Collin, Oxidative stress and the amyloid beta peptide in Alzheimer's disease, Redox Biology 14 (2018) 450-464. https://doi.org/https://doi.org/10.1016/j.redox.2017.10.014.
[3] B. Alies, E. Renaglia, M. Rózga, W. Bal, P. Faller, C. Hureau, Cu(II) Affinity for the Alzheimer's Peptide: Tyrosine Fluorescence Studies Revisited, Anal. Chem. 85 (2013) 1501-1508. https://doi.org/10.1021/ac302629u.
[4] C. Hureau, P. Dorlet, Coordination of redox active metal ions to the amyloid precursor protein and to amyloid-β peptides involved in Alzheimer disease. Part 2: Dependence of Cu(II) binding sites with Aβ sequences, Coord. Chem. Rev. 256 (2012) 2175-2187. https://doi.org/https://doi.org/10.1016/j.ccr.2012.03.034.
[5] J. Shearer, V.A. Szalai, The amyloid-beta peptide of Alzheimer's disease binds Cu(I) in a linear bis-his coordination environment: insight into a possible neuroprotective mechanism for the amyloid-beta peptide, J. Am. Chem. Soc. 130 (2008) 17826-17835. https://doi.org/10.1021/ja805940m.
[6] H. Atamna, W.H. Frey, 2nd, A role for heme in Alzheimer's disease: heme binds amyloid beta and has altered metabolism, Proc. Natl. Acad. Sci. USA 101 (2004) 11153-11158. https://doi.org/10.1073/pnas.0404349101.
[7] H. Atamna, D.W. Killilea, A.N. Killilea, B.N. Ames, Heme deficiency may be a factor in the mitochondrial and neuronal decay of aging, Proc. Natl. Acad. Sci. USA 99 (2002) 14807-14812. https://doi.org/10.1073/pnas.192585799.
[8] F. Sun, X. Mao, L. Xie, D.A. Greenberg, K. Jin, Neuroglobin protein is upregulated in Alzheimer's disease, J. Alzheimers Dis. 36 (2013) 659-663. https://doi.org/10.3233/JAD-130323.
[9] C.W. Wu, P.C. Liao, L. Yu, S.T. Wang, S.T. Chen, C.M. Wu, Y.M. Kuo, Hemoglobin promotes Abeta oligomer formation and localizes in neurons and amyloid deposits, Neurobiol. Dis. 17 (2004) 367-377. https://doi.org/10.1016/j.nbd.2004.08.014.
[10] H. Atamna, K. Boyle, Amyloid-beta peptide binds with heme to form a peroxidase: relationship to the cytopathologies of Alzheimer's disease, Proc. Natl. Acad. Sci. USA 103 (2006) 3381-3386. https://doi.org/10.1073/pnas.0600134103.
[11] H. Atamna, W.H. Frey, 2nd, N. Ko, Human and rodent amyloid-beta peptides differentially bind heme: relevance to the human susceptibility to Alzheimer's disease, Arch. Biochem. Biophys. 487 (2009) 59-65. https://doi.org/10.1016/j.abb.2009.05.003.
[12] Q. Bao, Y. Luo, W. Li, X. Sun, C. Zhu, P. Li, Z.X. Huang, X. Tan, The mechanism for heme to prevent Abeta(1-40) aggregation and its cytotoxicity, J. Biol. Inorg. Chem. 16 (2011) 809-816. https://doi.org/10.1007/s00775-011-0783-x.
[13] D. Pramanik, S.G. Dey, Active site environment of heme-bound amyloid beta peptide associated with Alzheimer's disease, J. Am. Chem. Soc. 133 (2011) 81-87. https://doi.org/10.1021/ja1084578.
[14] M. Roy, I. Pal, A.K. Nath, S.G. Dey, Peroxidase activity of heme bound amyloid beta peptides associated with Alzheimer's disease, Chem. Commun. 56 (2020) 4505-4518. https://doi.org/10.1039/c9cc09758a.
[15] G. Thiabaud, S. Pizzocaro, R. Garcia-Serres, J.-M. Latour, E. Monzani, L. Casella, Heme Binding Induces Dimerization and Nitration of Truncated β-Amyloid Peptide Aβ16 Under Oxidative Stress,

Angew. Chem. Int. Ed. 52 (2013) 8041-8044. https://doi.org/https://doi.org/10.1002/anie.201302989.
[16] S. Mukherjee, M. Seal, S.G. Dey, Kinetics of serotonin oxidation by heme-Abeta relevant to Alzheimer's disease, J. Biol. Inorg. Chem. 19 (2014) 1355-1365. https://doi.org/10.1007/s00775-014-1193-7.
[17] B. Neumann, A. Yarman, U. Wollenberger, F. Scheller, Characterization of the enhanced peroxidatic activity of amyloid beta peptide-hemin complexes towards neurotransmitters, Anal. Bioanal. Chem. 406 (2014) 3359-3364. https://doi.org/10.1007/s00216-014-7822-8.
[18] C. Yuan, H. Li, Z. Gao, Amyloid beta modulated the selectivity of heme-catalyzed protein tyrosine nitration: an alternative mechanism for selective protein nitration, J. Biol. Inorg. Chem. 17 (2012) 1083-1091. https://doi.org/10.1007/s00775-012-0922-z.
[19] C. Yuan, L. Yi, Z. Yang, Q. Deng, Y. Huang, H. Li, Z. Gao, Amyloid beta-heme peroxidase promoted protein nitrotyrosination: relevance to widespread protein nitration in Alzheimer's disease, J. Biol. Inorg. Chem. 17 (2012) 197-207. https://doi.org/10.1007/s00775-011-0842-3.
[20] A.K. Nath, C. Ghosh, M. Roy, M. Seal, S. Ghosh Dey, Nitrite reductase activity of heme and copper bound Aβ peptides, Dalton Trans. 48 (2019) 7451-7461. https://doi.org/10.1039/C9DT00914K.
[21] N. Lu, J. Li, R. Tian, Y.Y. Peng, Key roles of Arg(5), Tyr(10) and his residues in Abeta-heme peroxidase: relevance to Alzheimer's disease, Biochem. Biophys. Res. Commun. 452 (2014) 676-681. https://doi.org/10.1016/j.bbrc.2014.08.130.
[22] A. Wissbrock, T. Kuhl, K. Silbermann, A.J. Becker, O. Ohlenschlager, D. Imhof, Synthesis and Evaluation of Amyloid beta Derived and Amyloid beta Independent Enhancers of the Peroxidase-like Activity of Heme, J. Med. Chem. 60 (2017) 373-385. https://doi.org/10.1021/acs.jmedchem.6b01432.
[23] C. Yuan, Z. Gao, Abeta interacts with both the iron center and the porphyrin ring of heme: mechanism of heme's action on Abeta aggregation and disaggregation, Chem. Res. Toxicol. 26 (2013) 262-269. https://doi.org/10.1021/tx300441e.
[24] V. Pirota, E. Monzani, S. Dell'Acqua, L. Casella, Interactions between heme and tau-derived R1 peptides: binding and oxidative reactivity, Dalton Trans. 45 (2016) 14343-14351. https://doi.org/10.1039/c6dt02183b.
[25] P. Faller, C. Hureau, P. Dorlet, P. Hellwig, Y. Coppel, F. Collin, B. Alies, Methods and techniques to study the bioinorganic chemistry of metal–peptide complexes linked to neurodegenerative diseases, Coord. Chem. Rev. 256 (2012) 2381-2396. https://doi.org/https://doi.org/10.1016/j.ccr.2012.03.015.
[26] T. Kowalik-Jankowska, M. Ruta, K. Wisniewska, L. Lankiewicz, Coordination abilities of the 1-16 and 1-28 fragments of beta-amyloid peptide towards copper(II) ions: a combined potentiometric and spectroscopic study, J. Inorg. Biochem. 95 (2003) 270-282. https://doi.org/10.1016/s0162-0134(03)00128-4.
[27] P. Dorlet, S. Gambarelli, P. Faller, C. Hureau, Pulse EPR spectroscopy reveals the coordination sphere of copper(II) ions in the 1-16 amyloid-beta peptide: a key role of the first two N-terminus residues, Angew. Chem. Int. Ed. 48 (2009) 9273-9276. https://doi.org/10.1002/anie.200904567.
[28] L. Guilloreau, L. Damian, Y. Coppel, H. Mazarguil, M. Winterhalter, P. Faller, Structural and thermodynamical properties of CuII amyloid-beta16/28 complexes associated with Alzheimer's disease, J. Biol. Inorg. Chem. 11 (2006) 1024-1038. https://doi.org/10.1007/s00775-006-0154-1.
[29] C.D. Syme, R.C. Nadal, S.E. Rigby, J.H. Viles, Copper binding to the amyloid-beta (Abeta) peptide associated with Alzheimer's disease: folding, coordination geometry, pH dependence, stoichiometry, and affinity of Abeta-(1-28): insights from a range of complementary spectroscopic techniques, J. Biol. Chem. 279 (2004) 18169-18177. https://doi.org/10.1074/jbc.M313572200.
[30] D. Pramanik, C. Ghosh, S.G. Dey, Heme-Cu bound abeta peptides: spectroscopic characterization, reactivity, and relevance to Alzheimer's disease, J. Am. Chem. Soc. 133 (2011) 15545-15552. https://doi.org/10.1021/ja204628b.

[31] S. Choi, T.G. Spiro, K.C. Langry, K.M. Smith, D.L. Budd, G.N. La Mar, Structural correlations and vinyl influences in resonance Raman spectra of protoheme complexes and proteins, J. Am. Chem. Soc. 104 (1982) 4345-4351. https://doi.org/10.1021/ja00380a006.
[32] S. Hu, K.M. Smith, T.G. Spiro, Assignment of Protoheme Resonance Raman Spectrum by Heme Labeling in Myoglobin, J. Am. Chem. Soc. 118 (1996) 12638-12646. https://doi.org/10.1021/ja962239e.
[33] N. Parthasarathi, C. Hansen, S. Yamaguchi, T.G. Spiro, Metalloporphyrin core size resonance Raman marker bands revisited: implications for the interpretation of hemoglobin photoproduct Raman frequencies, J. Am. Chem. Soc. 109 (1987) 3865-3871. https://doi.org/10.1021/ja00247a009.
[34] P.V. Argade, M. Sassardi, D.L. Rousseau, T. Inubushi, M. Ikeda-Saito, A. Lapidot, Confirmation of the assignment of the iron-histidine stretching mode in myoglobin, J. Am. Chem. Soc. 106 (1984) 6593-6596. https://doi.org/10.1021/ja00334a024.
[35] O. Bangcharoenpaurpong, K.T. Schomacker, P.M. Champion, Resonance Raman investigation of myoglobin and hemoglobin, J. Am. Chem. Soc. 106 (1984) 5688-5698. https://doi.org/10.1021/ja00331a045.
[36] A. Desbois, M. Lutz, R. Banerjee, Resonance Raman spectra of deoxyhemoproteins. Heme structure in relation to dioxygen binding, Biochim. Biophys. Acta 671 (1981) 177-183. https://doi.org/10.1016/0005-2795(81)90132-x.
[37] S. Franzen, S.G. Boxer, R.B. Dyer, W.H. Woodruff, Resonance Raman Studies of Heme Axial Ligation in H93G Myoglobin, J. Phys. Chem. B 104 (2000) 10359-10367. https://doi.org/10.1021/jp001231v.
[38] J. Kincaid, P. Stein, T.G. Spiro, Absence of heme-localized strain in T state hemoglobin: insensitivity of heme-imidazole resonance Raman frequencies to quaternary structure, Proc. Natl. Acad. Sci. USA 76 (1979) 549-552. https://doi.org/10.1073/pnas.76.2.549.
[39] T. Kitagawa, K. Nagai, M. Tsubaki, Assignment of the Fe-Nepsilon (His F8) stretching band in the resonance Raman spectra of deoxy myoglobin, FEBS Lett. 104 (1979) 376-378. https://doi.org/10.1016/0014-5793(79)80856-x.
[40] S. Othman, A. Le Lirzin, A. Desbois, A heme c-peptide model system for the resonance Raman study of c-type cytochromes: characterization of the solvent-dependence of peptide-histidine-heme interactions, Biochemistry 32 (1993) 9781-9791. https://doi.org/10.1021/bi00088a033.
[41] S.S. Stavrov, The effect of iron displacement out of the porphyrin plane on the resonance Raman spectra of heme proteins and iron porphyrins, Biophys. J. 65 (1993) 1942-1950. https://doi.org/10.1016/S0006-3495(93)81265-7.
[42] J. Teraoka, T. Kitagawa, Resonance Raman study of the heme-linked ionization in reduced horseradish peroxidase, Biochem. Biophys. Res. Commun. 93 (1980) 694-700. https://doi.org/10.1016/0006-291x(80)91133-x.
[43] A.V. Wells, J.T. Sage, D. Morikis, P.M. Champion, M.L. Chiu, S.G. Sligar, The iron-histidine mode of myoglobin revisited: resonance Raman studies of isotopically labeled Escherichia coli-expressed myoglobin, J. Am. Chem. Soc. 113 (1991) 9655-9660. https://doi.org/10.1021/ja00025a034.
[44] A. Desbois, M. Lutz, Low-frequency vibrations of ferroprotoporphyrin-substituted imidazole complexes. A resonance Raman study, Biochim. Biophys. Acta 671 (1981) 168-176. https://doi.org/https://doi.org/10.1016/0005-2795(81)90131-8.
[45] A. Desbois, M. Lutz, Redox control of proton transfers in membrane b-type cytochromes: an absorption and resonance Raman study on bis(imidazole) and bis(imidazolate) model complexes of iron-protoporphyrin, Eur. Biophys. J. 20 (1992) 321-335. https://doi.org/10.1007/BF00196591.
[46] M.L. Mitchell, X.Y. Li, J.R. Kincaid, T.G. Spiro, Axial ligand and out-of-plane vibrations for bis(imidazolyl)heme: Raman and infrared iron-54, nitrogen-15, and deuterium isotope shifts and normal coordinate calculations, J. Phys. Chem. 91 (1987) 4690-4696. https://doi.org/10.1021/j100302a013.

[47] M.C. Silvestrini, M. Tegoni, J. Celerier, A. Desbois, M. Gervais, Expression in Escherichia coli of the flavin and the haem domains of Hansenula anomala flavocytochrome b2 (flavodehydrogenase and b2 core) and characterization of the recombinant proteins, Biochem. J 295 ( Pt 2) (1993) 501-508. https://doi.org/10.1042/bj2950501.
[48] X.Y. Li, T.G. Spiro, Is bound carbonyl linear or bent in heme proteins? Evidence from resonance Raman and infrared spectroscopic data, J. Am. Chem. Soc. 110 (1988) 6024-6033. https://doi.org/10.1021/ja00226a017.
[49] T.G. Spiro, A.V. Soldatova, G. Balakrishnan, CO, NO and O2 as Vibrational Probes of Heme Protein Interactions, Coord. Chem. Rev. 257 (2013) 511-527. https://doi.org/10.1016/j.ccr.2012.05.008.
[50] T.G. Spiro, I.H. Wasbotten, CO as a vibrational probe of heme protein active sites, J. Inorg. Biochem. 99 (2005) 34-44. https://doi.org/10.1016/j.jinorgbio.2004.09.026.
[51] K.M. Vogel, P.M. Kozlowski, M.Z. Zgierski, T.G. Spiro, Role of the axial ligand in heme·CO backbonding; DFT analysis of vibrational data, Inorg. Chim. Acta 297 (2000) 11-17. https://doi.org/https://doi.org/10.1016/S0020-1693(99)00253-4.
[52] N.T. Yu, E.A. Kerr, B. Ward, C.K. Chang, Resonance Raman detection of Fe-CO stretching and Fe-C-O bending vibrations in sterically hindered carbonmonoxy "strapped hemes". A structural probe of Fe-C-O distortion, Biochemistry 22 (1983) 4534-4540. https://doi.org/10.1021/bi00288a028.
[53] A. Desbois, G. Mazza, F. Stetzkowski, M. Lutz, Resonance raman spectroscopy of protoheme-protein interactions in oxygen-carrying hemoproteins and in peroxidases, Biochim. Biophys. Acta 785 (1984) 161-176. https://doi.org/https://doi.org/10.1016/0167-4838(84)90140-7.
[54] Y. Bin, S. Chen, J. Xiang, pH-dependent kinetics of copper ions binding to amyloid-beta peptide, J. Inorg. Biochem. 119 (2013) 21-27. https://doi.org/10.1016/j.jinorgbio.2012.10.013.
[55] J. Lindgren, P. Segerfeldt, S.B. Sholts, A. Graslund, A.E. Karlstrom, S.K. Warmlander, Engineered non-fluorescent Affibody molecules facilitate studies of the amyloid-beta (Abeta) peptide in monomeric form: low pH was found to reduce Abeta/Cu(II) binding affinity, J. Inorg. Biochem. 120 (2013) 18-23. https://doi.org/10.1016/j.jinorgbio.2012.11.005.
[56] Y. El Khoury, P. Dorlet, P. Faller, P. Hellwig, New insights into the coordination of Cu(II) by the amyloid-B 16 peptide from Fourier transform IR spectroscopy and isotopic labeling, J. Phys. Chem. B 115 (2011) 14812-14821. https://doi.org/10.1021/jp207328y.
[57] S. Furlan, C. Hureau, P. Faller, G. La Penna, Modeling copper binding to the amyloid-beta peptide at different pH: toward a molecular mechanism for Cu reduction, J. Phys. Chem. B 116 (2012) 11899-11910. https://doi.org/10.1021/jp308977s.
[58] J.W. Karr, H. Akintoye, L.J. Kaupp, V.A. Szalai, N-Terminal deletions modify the Cu2+ binding site in amyloid-beta, Biochemistry 44 (2005) 5478-5487. https://doi.org/10.1021/bi047611e.
[59] B.K. Shin, S. Saxena, Substantial contribution of the two imidazole rings of the His13-His14 dyad to Cu(II) binding in amyloid-beta(1-16) at physiological pH and its significance, J. Phys. Chem. A 115 (2011) 9590-9602. https://doi.org/10.1021/jp200379m.
[60] A. Boffi, T.K. Das, S. della Longa, C. Spagnuolo, D.L. Rousseau, Pentacoordinate hemin derivatives in sodium dodecyl sulfate micelles: model systems for the assignment of the fifth ligand in ferric heme proteins, Biophys. J. 77 (1999) 1143-1149. https://doi.org/10.1016/S0006-3495(99)76965-1.
[61] D.L. Rousseau, Y.C. Ching, M. Brunori, G.M. Giacometti, Axial coordination of ferric Aplysia myoglobin, J. Biol. Chem. 264 (1989) 7878-7881.
[62] S. Dasgupta, D.L. Rousseau, H. Anni, T. Yonetani, Structural characterization of cytochrome c peroxidase by resonance Raman scattering, J. Biol. Chem. 264 (1989) 654-662. https://doi.org/10.1016/S0021-9258(17)31311-X.
[63] V. Palaniappan, J. Terner, Resonance Raman spectroscopy of horseradish peroxidase derivatives and intermediates with excitation in the near ultraviolet, J. Biol. Chem. 264 (1989) 16046-16053.
[64] C. Ghosh, M. Seal, S. Mukherjee, S. Ghosh Dey, Alzheimer's Disease: A Heme–Aβ Perspective, Acc. Chem. Res. 48 (2015) 2556-2564. https://doi.org/10.1021/acs.accounts.5b00102.

[65] D. Pramanik, C. Ghosh, S. Mukherjee, S.G. Dey, Interaction of amyloid β peptides with redox active heme cofactor: Relevance to Alzheimer's disease, Coord. Chem. Rev. 257 (2013) 81-92. https://doi.org/https://doi.org/10.1016/j.ccr.2012.02.025.
[66] S.A. Kotler, P. Walsh, J.R. Brender, A. Ramamoorthy, Differences between amyloid-beta aggregation in solution and on the membrane: insights into elucidation of the mechanistic details of Alzheimer's disease, Chem. Soc. Rev. 43 (2014) 6692-6700. https://doi.org/10.1039/c3cs60431d.
[67] J. Simplicio, Hemin monomers in micellar sodium lauryl sulfate. A spectral and equilibrium study with cyanide, Biochemistry 11 (1972) 2525-2528. https://doi.org/10.1021/bi00763a022.
[68] D. Keilin, E.F. Hartree, Purification of horse-radish peroxidase and comparison of its properties with those of catalase and methaemoglobin, Biochem. J. 49 (1951) 88-104. https://doi.org/10.1042/bj0490088.
[69] J.A. Manthey, N.J. Boldt, D.F. Bocian, S.I. Chan, Resonance Raman studies of lactoperoxidase, J. Biol. Chem. 261 (1986) 6734-6741.
[70] Y.A. Sharonov, Evidence for the high-spin heme iron in both stable and unstable reduced forms of lactoperoxidase: low-temperature magnetic circular dichroism data, FEBS Lett. 377 (1995) 512-514. https://doi.org/10.1016/0014-5793(95)01409-8.
[71] J. Teraoka, T. Kitagawa, Structural implication of the heme-linked ionization of horseradish peroxidase probed by the Fe-histidine stretching Raman line, J. Biol. Chem. 256 (1981) 3969-3977.
[72] E.B. Draganova, N. Akbas, S.A. Adrian, G.S. Lukat-Rodgers, D.P. Collins, J.H. Dawson, C.E. Allen, M.P. Schmitt, K.R. Rodgers, D.W. Dixon, Heme Binding by Corynebacterium diphtheriae HmuT: Function and Heme Environment, Biochemistry 54 (2015) 6598-6609. https://doi.org/10.1021/acs.biochem.5b00666.
[73] S. Othman, P. Richaud, A. Vermeglio, A. Desbois, Evidence for a proximal histidine interaction in the structure of cytochromes c in solution: a resonance Raman study, Biochemistry 35 (1996) 9224-9234. https://doi.org/10.1021/bi952818g.
[74] M. Ibrahim, C. Xu, T.G. Spiro, Differential sensing of protein influences by NO and CO vibrations in heme adducts, J. Am. Chem. Soc. 128 (2006) 16834-16845. https://doi.org/10.1021/ja064859d.
[75] D.P. Linder, N.J. Silvernail, A. Barabanschikov, J. Zhao, E.E. Alp, W. Sturhahn, J.T. Sage, W.R. Scheidt, K.R. Rodgers, The diagnostic vibrational signature of pentacoordination in heme carbonyls, J. Am. Chem. Soc. 136 (2014) 9818-9821. https://doi.org/10.1021/ja503191z.
[76] P.J. Mak, M.C. Gregory, S.G. Sligar, J.R. Kincaid, Resonance Raman spectroscopy reveals that substrate structure selectively impacts the heme-bound diatomic ligands of CYP17, Biochemistry 53 (2014) 90-100. https://doi.org/10.1021/bi4014424.
[77] A. Sato, Y. Sasakura, S. Sugiyama, I. Sagami, T. Shimizu, Y. Mizutani, T. Kitagawa, Stationary and time-resolved resonance Raman spectra of His77 and Met95 mutants of the isolated heme domain of a direct oxygen sensor from Escherichia coli, J. Biol. Chem. 277 (2002) 32650-32658. https://doi.org/10.1074/jbc.M204559200.
[78] Y. Sun, W. Zeng, A. Benabbas, X. Ye, I. Denisov, S.G. Sligar, J. Du, J.H. Dawson, P.M. Champion, Investigations of heme ligation and ligand switching in cytochromes p450 and p420, Biochemistry 52 (2013) 5941-5951. https://doi.org/10.1021/bi400541v.
[79] K. Tang, M. Knipp, B.B. Liu, N. Cox, R. Stabel, Q. He, M. Zhou, H. Scheer, K.H. Zhao, W. Gartner, Redox-dependent Ligand Switching in a Sensory Heme-binding GAF Domain of the Cyanobacterium Nostoc sp. PCC7120, J. Biol. Chem. 290 (2015) 19067-19080. https://doi.org/10.1074/jbc.M115.654087.
[80] T. Uchida, E. Sato, A. Sato, I. Sagami, T. Shimizu, T. Kitagawa, CO-dependent activity-controlling mechanism of heme-containing CO-sensor protein, neuronal PAS domain protein 2, J. Biol. Chem. 280 (2005) 21358-21368. https://doi.org/10.1074/jbc.M412350200.
[81] X. Ye, A. Yu, G.Y. Georgiev, F. Gruia, D. Ionascu, W. Cao, J.T. Sage, P.M. Champion, CO rebinding to protoheme: investigations of the proximal and distal contributions to the geminate rebinding barrier, J. Am. Chem. Soc. 127 (2005) 5854-5861. https://doi.org/10.1021/ja042365f.

[82] A. Brunel, A. Wilson, L. Henry, P. Dorlet, J. Santolini, The proximal hydrogen bond network modulates *Bacillus subtilis* nitric-oxide synthase electronic and structural properties, J. Biol. Chem. 286 (2011) 11997-12005. https://doi.org/10.1074/jbc.M110.195446.
[83] S.D. Carson, I. Constantinidis, J.D. Satterlee, M.R. Ondrias, A resonance Raman study of ligand binding geometry in Glycera dibranchiata carbonmonoxyhemoglobin, J. Biol. Chem. 260 (1985) 8741-8745. https://doi.org/10.1016/S0021-9258(17)39414-0.
[84] C.M. Coyle, K.M. Vogel, T.S. Rush, 3rd, P.M. Kozlowski, R. Williams, T.G. Spiro, Y. Dou, M. Ikeda-Saito, J.S. Olson, M.Z. Zgierski, FeNO structure in distal pocket mutants of myoglobin based on resonance Raman spectroscopy, Biochemistry 42 (2003) 4896-4903. https://doi.org/10.1021/bi026395b.
[85] S. Han, D.L. Rousseau, G. Giacometti, M. Brunori, Metastable intermediates in myoglobin at low pH, Proc. Natl. Acad. Sci. USA 87 (1990) 205-209. https://doi.org/10.1073/pnas.87.1.205.
[86] A. Ioanoviciu, E.T. Yukl, P. Moenne-Loccoz, P.R. de Montellano, DevS, a heme-containing two-component oxygen sensor of Mycobacterium tuberculosis, Biochemistry 46 (2007) 4250-4260. https://doi.org/10.1021/bi602422p.
[87] T. Li, M.L. Quillin, G.N. Phillips, Jr., J.S. Olson, Structural determinants of the stretching frequency of CO bound to myoglobin, Biochemistry 33 (1994) 1433-1446. https://doi.org/10.1021/bi00172a021.
[88] Y. Liu, P. Moenne-Loccoz, D.P. Hildebrand, A. Wilks, T.M. Loehr, A.G. Mauk, P.R. Ortiz de Montellano, Replacement of the proximal histidine iron ligand by a cysteine or tyrosine converts heme oxygenase to an oxidase, Biochemistry 38 (1999) 3733-3743. https://doi.org/10.1021/bi982707s.
[89] H. Miyatake, M. Mukai, S. Adachi, H. Nakamura, K. Tamura, T. Iizuka, Y. Shiro, R.W. Strange, S.S. Hasnain, Iron coordination structures of oxygen sensor FixL characterized by Fe K-edge extended x-ray absorption fine structure and resonance raman spectroscopy, J. Biol. Chem. 274 (1999) 23176-23184. https://doi.org/10.1074/jbc.274.33.23176.
[90] G.N. Phillips, M.L. Teodoro, T. Li, B. Smith, J.S. Olson, Bound CO Is A Molecular Probe of Electrostatic Potential in the Distal Pocket of Myoglobin, J. Phys. Chem. B 103 (1999) 8817-8829. https://doi.org/10.1021/jp9918205.
[91] J. Ramsden, T.G. Spiro, Resonance Raman evidence that distal histidine protonation removes the steric hindrance to upright binding of carbon monoxide by myoglobin, Biochemistry 28 (1989) 3125-3128. https://doi.org/10.1021/bi00434a001.
[92] W. Gong, B. Hao, S.S. Mansy, G. Gonzalez, M.A. Gilles-Gonzalez, M.K. Chan, Structure of a biological oxygen sensor: a new mechanism for heme-driven signal transduction, Proc. Natl. Acad. Sci. USA 95 (1998) 15177-15182. https://doi.org/10.1073/pnas.95.26.15177.
[93] E.A. Padlan, W.E. Love, Three-dimensional structure of hemoglobin from the polychaete annelid, Glycera dibranchiata, at 2.5 A resolution, J. Biol. Chem. 249 (1974) 4067-4078.
[94] H.A. Feaga, R.C. Maduka, M.N. Foster, V.A. Szalai, Affinity of Cu+ for the copper-binding domain of the amyloid-beta peptide of Alzheimer's disease, Inorg. Chem. 50 (2011) 1614-1618. https://doi.org/10.1021/ic100967s.
[95] C. Hureau, V. Balland, Y. Coppel, P.L. Solari, E. Fonda, P. Faller, Importance of dynamical processes in the coordination chemistry and redox conversion of copper amyloid-beta complexes, J. Biol. Inorg. Chem. 14 (2009) 995-1000. https://doi.org/10.1007/s00775-009-0570-0.
[96] Y. El Khoury, A. Schirer, C. Patte-Mensah, C. Klein, L. Meyer, M. Rataj-Baniowska, S. Bernad, D. Moss, S. Lecomte, A.G. Mensah-Nyagan, P. Hellwig, Raman Imaging Reveals Accumulation of Hemoproteins in Plaques from Alzheimer's Diseased Tissues, ACS Chem. Neurosci. (2021) https://doi.org/10.1021/acschemneuro.1c00289.

**Table 1.** Observed frequencies (cm $^{-1}$) of selected RR modes of Aβ40- and Aβ16- FePP complexes.

| Modes | Fe(III)PP complexes (pH 6.7) | | Fe(II)PP complexes (pH 7.4) | | Fe(II)PPCO complexes (pH 7.4) | |
|---|---|---|---|---|---|---|
| | Aβ40 6cLS 5cHS | Aβ16 6cLS 5cHS | Aβ40 6cLS 5cHS | Aβ16 6cLS 5cHS | Aβ40 6cLS 5cHS | Aβ16 6cLS 5cHS |
| **ν(C=O)** | - | - | - | - | 1964/1957 | 1963/1956 |
| **$\nu_{10}$** | 1640/1626 | 1641/1627 | 1617/1602 | 1617/1603 | 1630/1603* | 1630/1602* |
| **$\nu(C_a{=}C_b)_{Vn}$** | 1621 | 1620 | 1621 | 1621 | 1621 | 1622 |
| **$\nu_2$** | 1580/1570 | 1580/1571 | 1581/1561 | 1581/1560 | 1583/1562* | 1583/1561* |
| **$\nu_{11}$** | 1562/1556 | 1561/1555 | 1532/1545 | 1532/1547 | 1555/1545* | 1556/1545* |
| **$\nu_3$** | 1505/1490 | 1505/1491 | 1496/1469 | 1497/1469 | 1501/1469* | 1501/1470* |
| **$\delta(=C_bH_2)_{Vn}$** | 1452 | 1453 | 1450 | 1453 | 1450 | 1451 |
| **$\delta(=C_bH_2)_{Vn}$** | 1430 | 1431 | 1430 | 1429 | 1431 | 1431 |
| **$\nu_4$** | 1373/1372 | 1373/1372 | 1366/1357 | 1367/1356 | 1372/1357* | 1372/1357* |
| **$\delta(C_aH{=})_{Vn}$** | 1311 | 1311 | 1311 | 1312 | 1312 | 1311 |
| **$\delta(C_aH{=})_{Vn}$** | 1304 | 1302 | 1304 | 1305 | 1305 | 1305 |
| **$\nu(C_\beta\text{-}C)_{Me}$ ($\nu_{14}$)** | 1128 | 1126 | 1129 | 1130 | 1132 | 1132 |
| **$(\nu(C_\beta\text{-}C)_{Me}$ ($\nu_5$)** | 1119 | 1118 | 1120 | 1120 | 1123 | 1123 |
| **$\nu(C_\beta\text{-}C)_{Vn}$ ($\nu_{45}$)** | 1005 | 1005 | 1006 | 1005 | 1005 | 1006 |
| **$\nu_7$** | 677/675 | 677/675 | 675 | 675 | 677 | 677 |
| **ν(Fe-CO)** | - | - | - | - | 526/496 | 529/496 |
| **$\delta(C_\beta C_a C_b)_{Vn}$** | 419/411 | 418/411 | 417/413 | 417/412 | 418/413* | 418/414* |
| **$\delta(C_\beta C_c C_d)_{Pr}$** | 381/377 | 381/378 | 381/378 | 379/374 | 383 | 382 |
| **$\nu$(Fe-$N_{Pyr}$) ($\nu_8$)** | 350/347 | 351/347 | 348/346 | 348/343 | 349 | 349 |
| **$\nu$(Fe-$N_{His}$)** | - | - | 221 | 225 | 222* | 225* |

* Photodissociated product

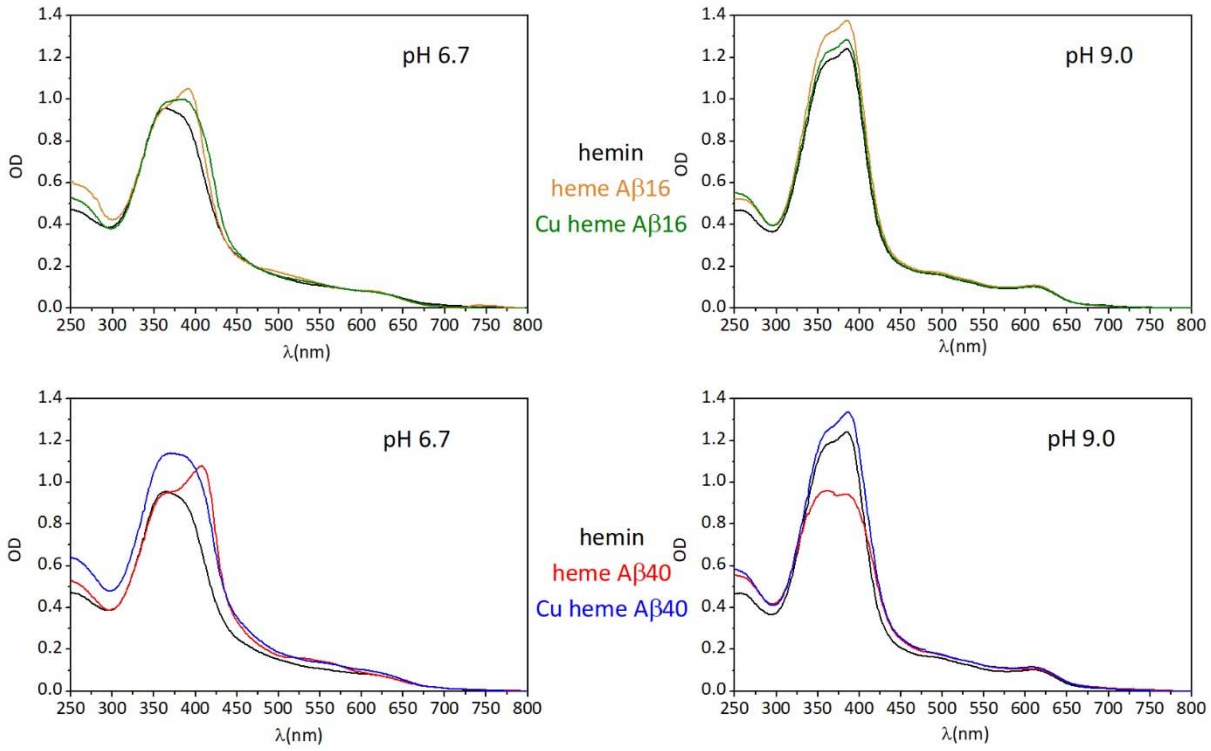


***Figure 1*.** UV-visible spectra of the complexes between heme and Aβ peptides at pH 6.7 (right panels) or 9.0 (left panels). Peptide, hemin and Cu concentrations: 200 µM.

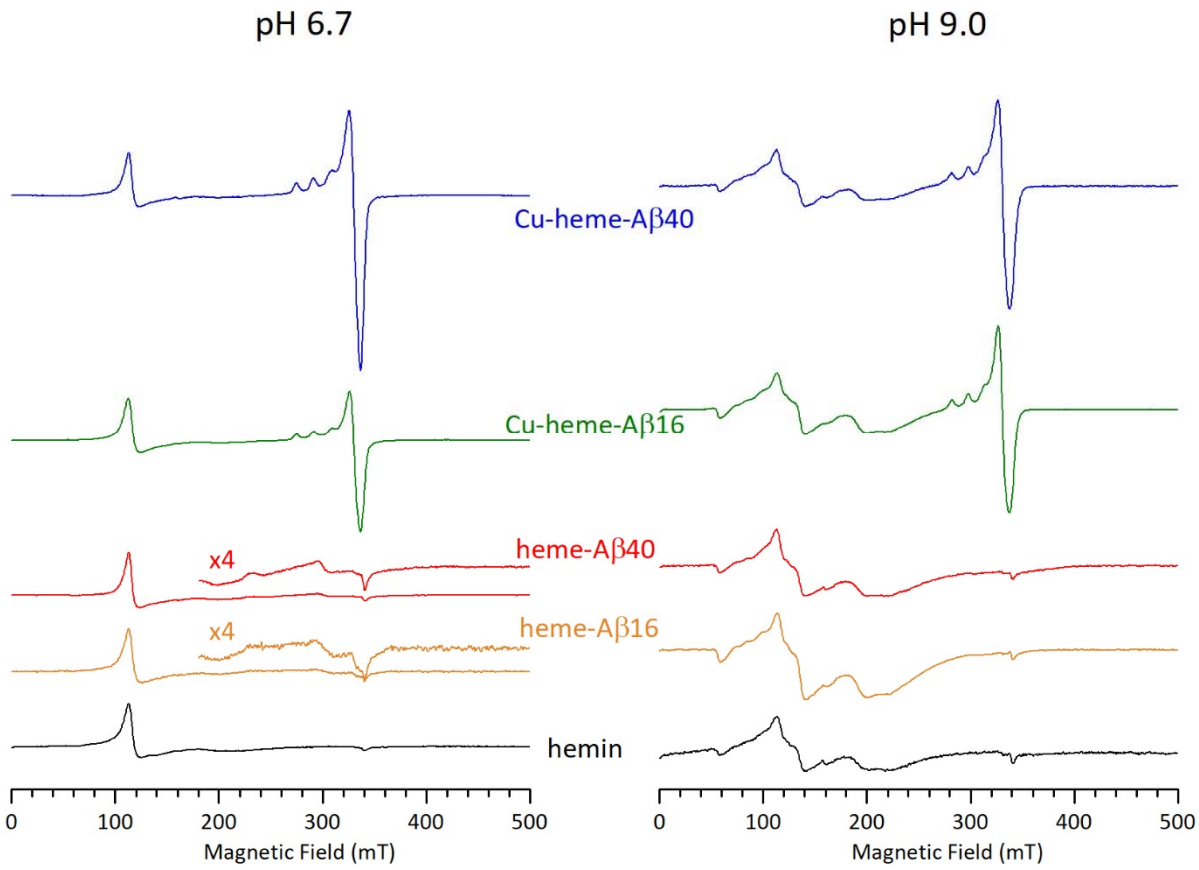


***Figure 2.*** EPR spectra of the complexes of Aβ with heme in the presence (top spectra) or in the absence (bottom spectra) of 1 equivalent of Cu(II) at pH 6.7 (left) and at pH 9 (right). Experimental conditions: microwave frequency 9.4956 GHz, field modulation amplitude 2 mT, microwave power 0.5 mW, T 10 K. Spectra have been baseline corrected and normalized on the high spin signal maximum for display.

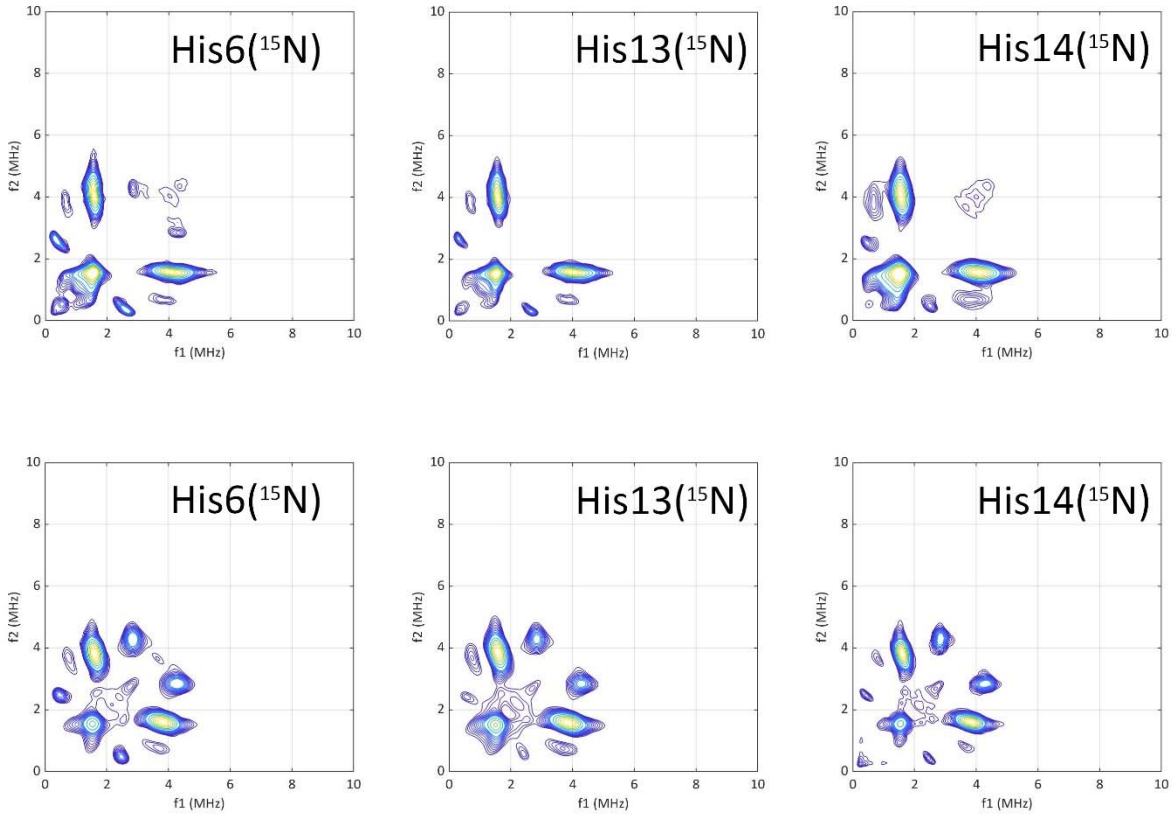


***Figure 3*.** 4-pulse HYSCORE contour plots for Aβ16-Cu(II)-heme complex at pH 6.5 (top spectra) and 9.0 (bottom spectra). The Aβ peptide was specifically labelled with $^{15}N$ on His6 (left panels), His13 (middle panel) or His14 (right panels). Experimental conditions: microwave frequency 9.66 GHz, B = 336 mT, T 4.2 K, τ = 136 ns.

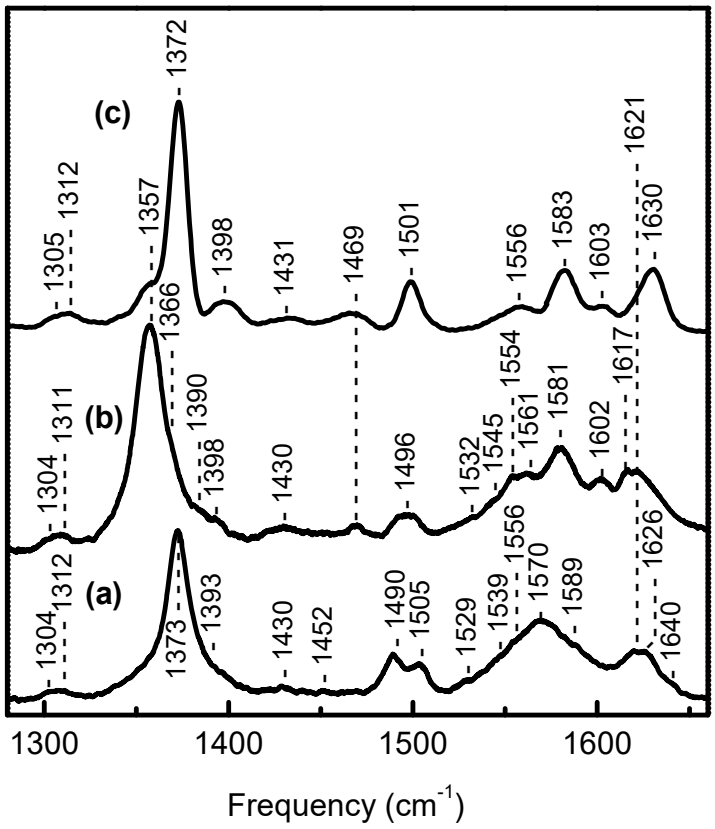


***Figure 4.*** High-frequency regions of RR spectra of Aβ40-FePP complexes at pH 6.7. (a) ferric form excited at 441.6 nm; (b) ferrous form excited at 441.6 nm; (c) ferrous carbonyl form excited at 413.1 nm .

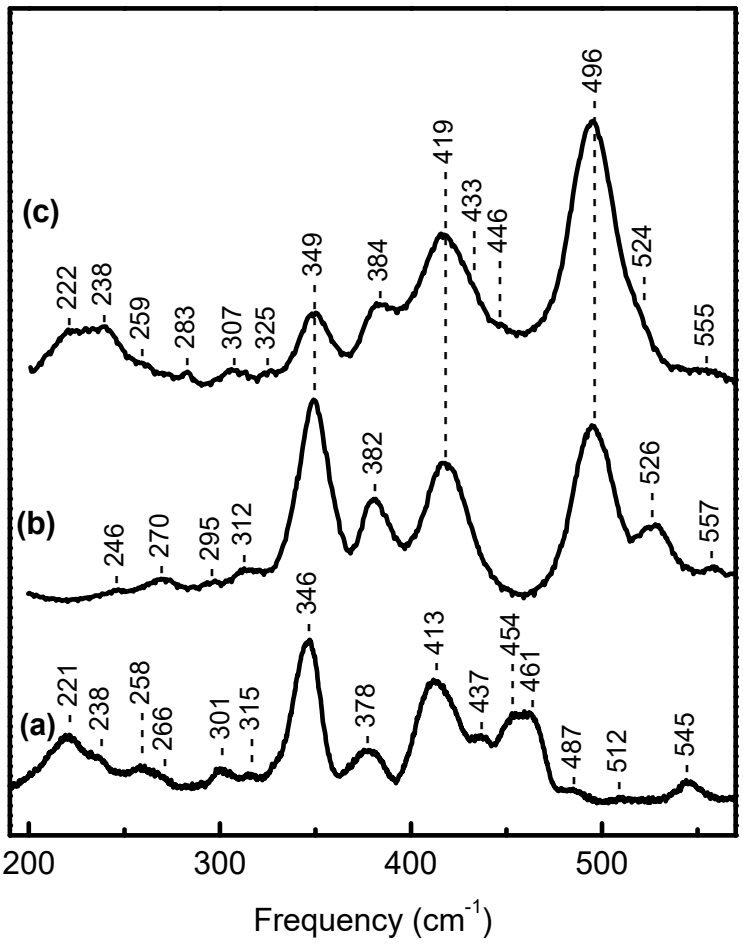


***Figure 5.*** Low-frequency regions (190-570 $cm^{-1}$) of RR spectra of ferroprotoheme (Fe(II)PP) complexes of Aβ40. (a) Aβ40-Fe(II)PP complex excited at 441.6 nm; (b) Aβ40-Fe(II)PPCO complex excited at 413.1 nm; (c) Aβ40-Fe(II)PPCO complex excited at 441.6 nm.

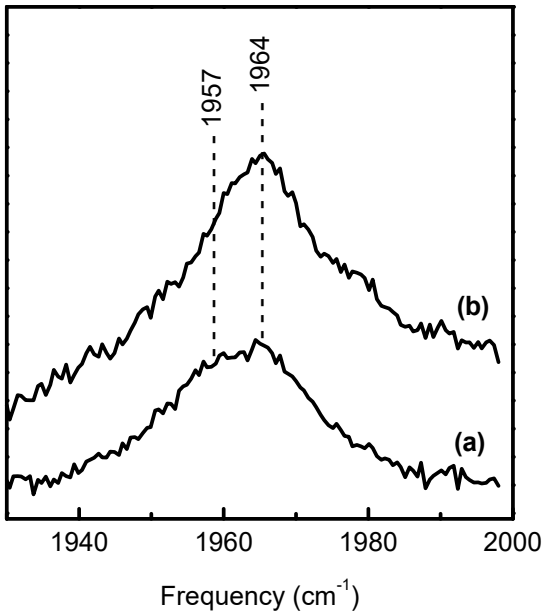


***Figure 6.*** ν(CO) regions of RR spectra of Aβ40-Fe(II)PPCO complexes excited at 413.1 (a) and 441.6 (b) nm.

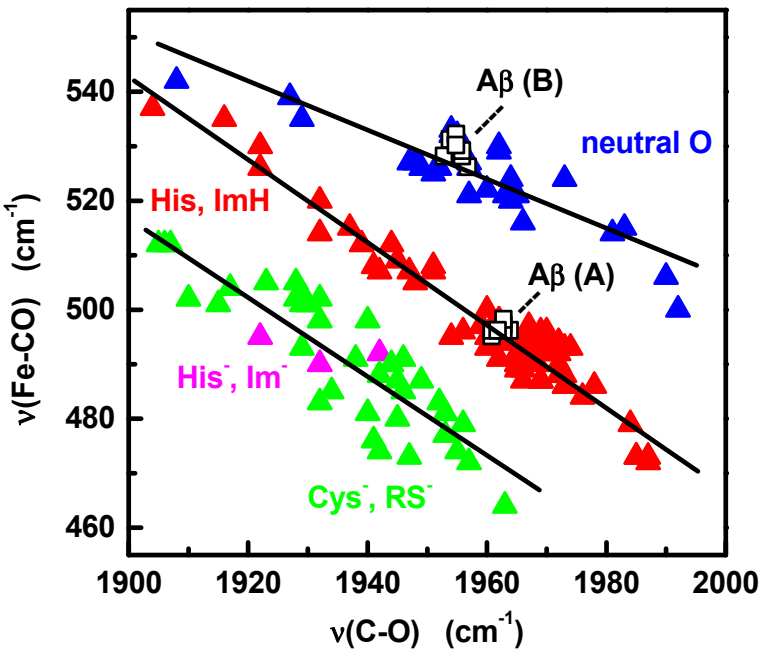


***Figure 7***. Plot of the observed frequencies of ν(Fe-CO) *vs* ν(CO) frequencies of CO derivatives of ferrous hemoproteins and model compounds. Red triangles: neutral N(imidazole) ligand; Magenta triangles: anionic N(imidazolate) ligand; Green triangles: anionic S(thiolate) ligand; Blue triangles: neutral O ligand. The open black squares represent the data obtained for the Aβ40- and Aβ16-Fe(II)PPCO complexes. The ν(FeCO) and ν(CO) frequencies are taken from references [48-52, 72, 74-91] and references cited therein.

## Supplementary Information

**Coordination of Fe-protoheme with amyloid β is non-specific and exhibits multiple equilibria**

Jérôme Gout,[2] Floriane Meuris,[2] Alain Desbois*[2] and Pierre Dorlet*[1, 2]

[1]CNRS, Aix Marseille Université, BIP, IMM, Marseille, France

[2]Université Paris-Saclay, CEA, CNRS, Institute for Integrative Biology of the Cell (I2BC), Laboratoire Stress Oxydant et Détoxication, Gif-sur-Yvette, France

*To whom correspondence should be addressed : alain.desbois@netcourrier.com, pdorlet@imm.cnrs.fr

**Table S1.** Observed Frequencies ($cm^{-1}$) of the ν(Fe-CO) and ν(Fe-CO) modes of Aβ-FePPCO complexes

| Complexes | ν(Fe-CO) A form | ν(Fe-CO) B form | ν(C=O) A form | ν(C=O) B form |
|---|---|---|---|---|
| Aβ16-Fe(II)PPCO pH 6.7 | 496 | 530 | 1962 | 1955 |
| Aβ16-Fe(II)PPCO pH 6.7 + Cu(I) (1eq/heme) | 495 | 531 | 1961 | 1954 |
| Aβ16-Fe(II)PPCO pH 7.4 | 496 | 529 | 1963 | 1956 |
| Aβ40-Fe(II)PPCO pH 7.4 | 496 | 526 | 1964 | 1957 |
| Aβ16-Fe(II)PPCO pH 9.0 | 496 | 532 | 1961 | 1955 |
| Aβ16-Fe(II)PPCO pH 9.0 + Cu(I) (1eq/heme) | 498 | 528 | 1963 | 1953 |

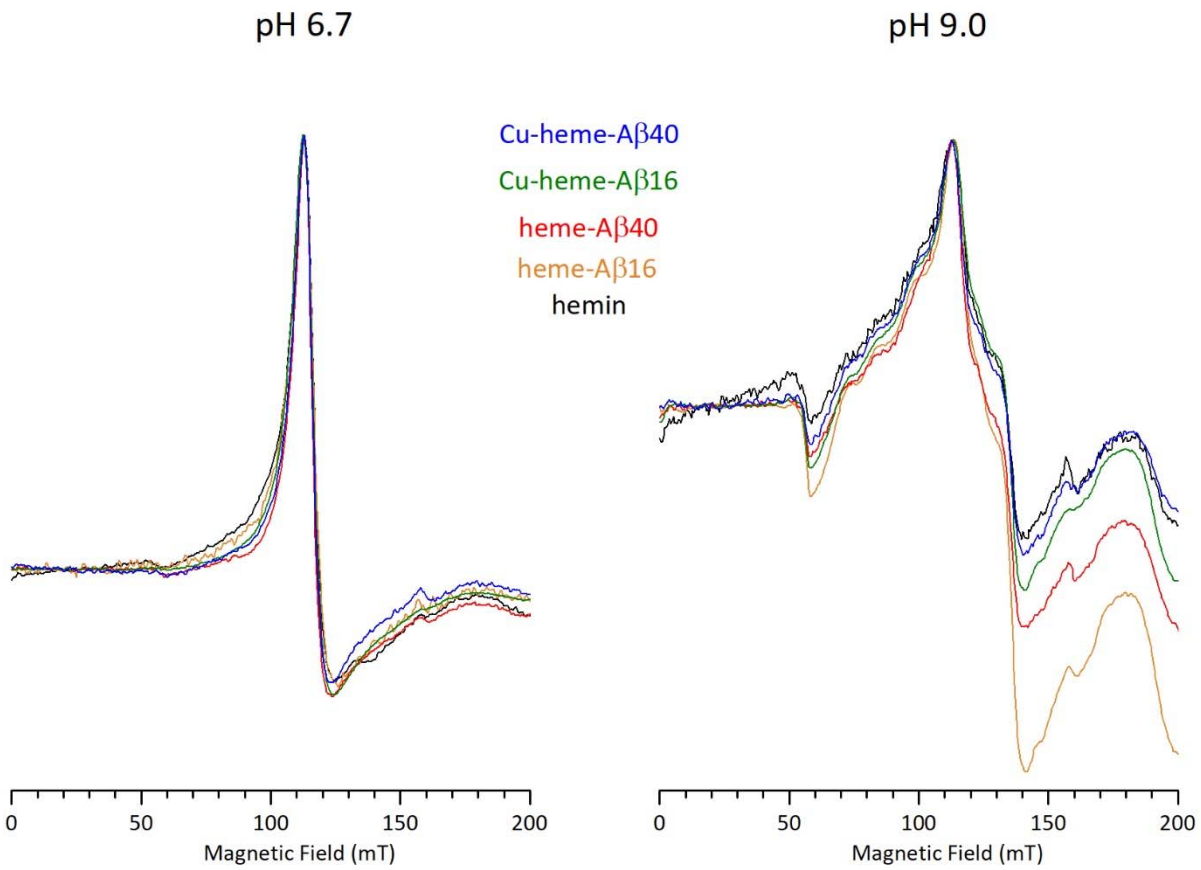


***Figure S1*.** Zoom on the low field/high spin region of the EPR spectra of the complexes of Aβ with heme in the presence or in the absence of 1 equivalent of Cu(II) at pH 6.7 (left) and at pH 9 (right). Experimental conditions: microwave frequency 9.4956 GHz, field modulation amplitude 2 mT, microwave power 0.5 mW, T 10 K. Spectra have been normalized on the high spin signal maximum.

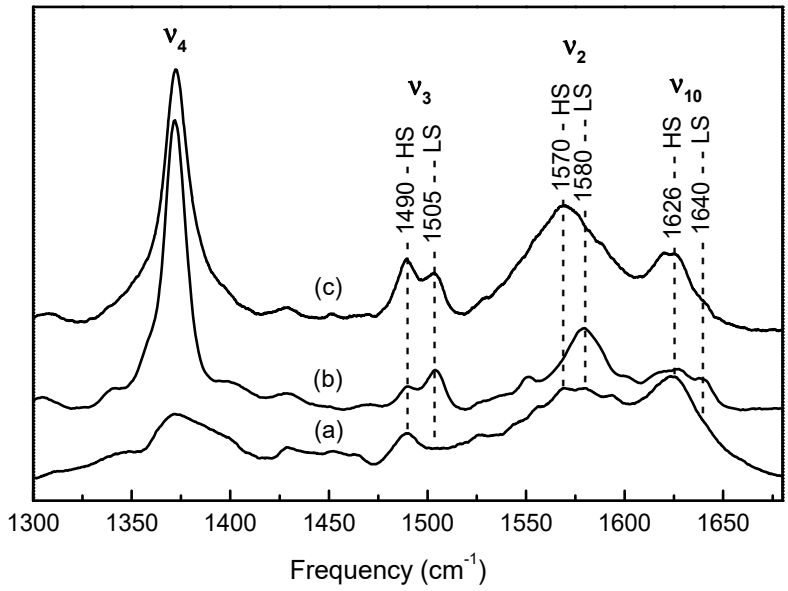


***Figure S2*.** High-frequency region of RR spectra of Aβ40-Fe(III)PP complex at pH 6.7. Excitation at (a) 363.8 nm, (b) 413.1 nm, and (c) 441.6 nm

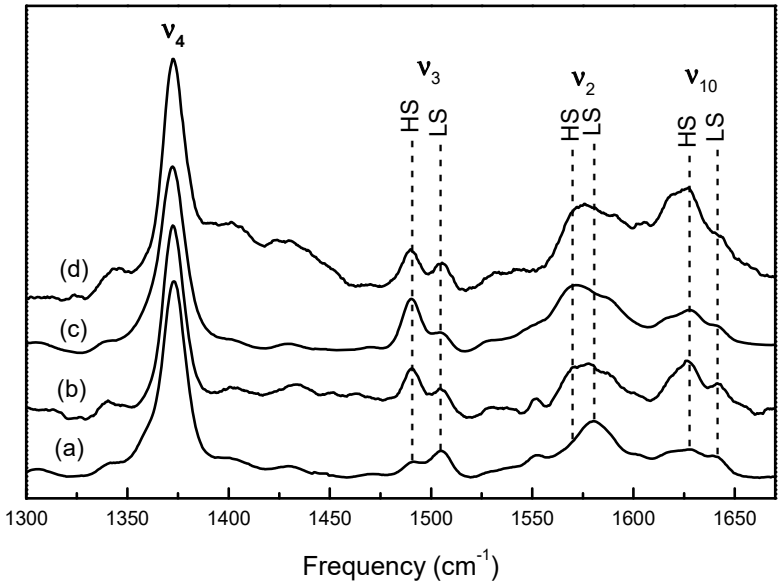


***Figure S3*.** High-frequency region of RR spectra of Aβ40- and Aβ16-Fe(III)PP complexes. (a) Aβ40, pH 6.7; (b) Aβ40, pH 9.0; (c) Aβ16, pH 6.7; (d) Aβ16, pH 9.0. Excitation: 413.1 nm

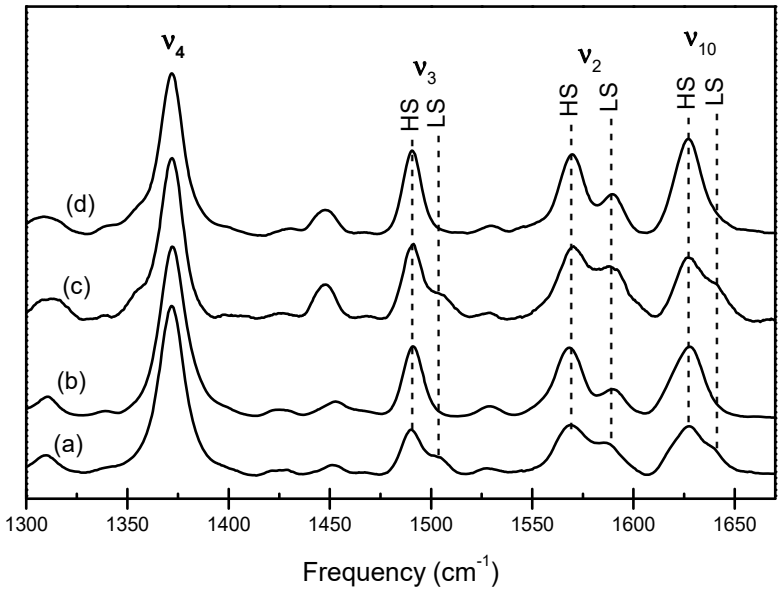


***Figure S4*.** High-frequency region of RR spectra of Aβ16-Fe(III)PP complexes. (a) pH 6.7; (b) pH 6.7 + 1 eq Cu(II); (c) pH 9.0; (d) pH 9.0 + 1 eq Cu(II). Excitation: 441.6 nm

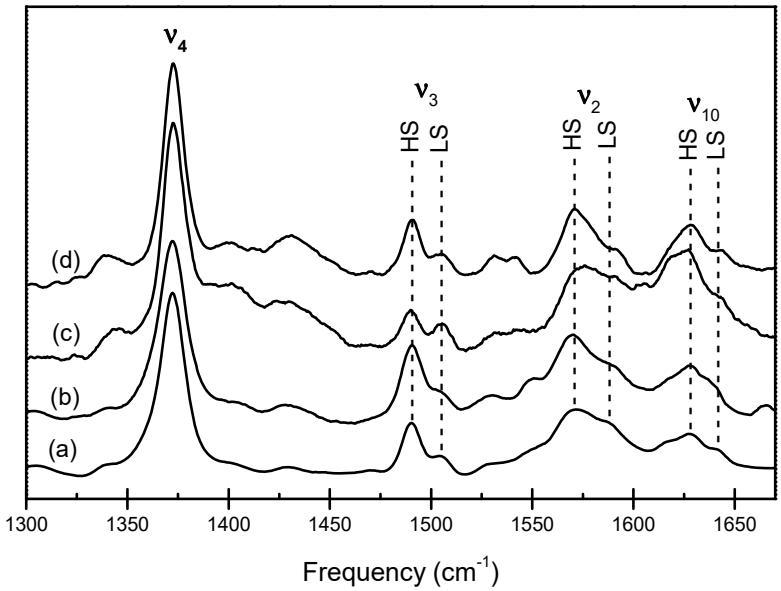


***Figure S5.*** High-frequency region of RR spectra of Aβ16-Fe(III)PP complexes (a) pH 6.7; (b) pH 6.7 + 1eq Cu(II); (c) pH 9.0; (d) pH 9.0 + 1 eq Cu(II). Excitation: 413.1 nm

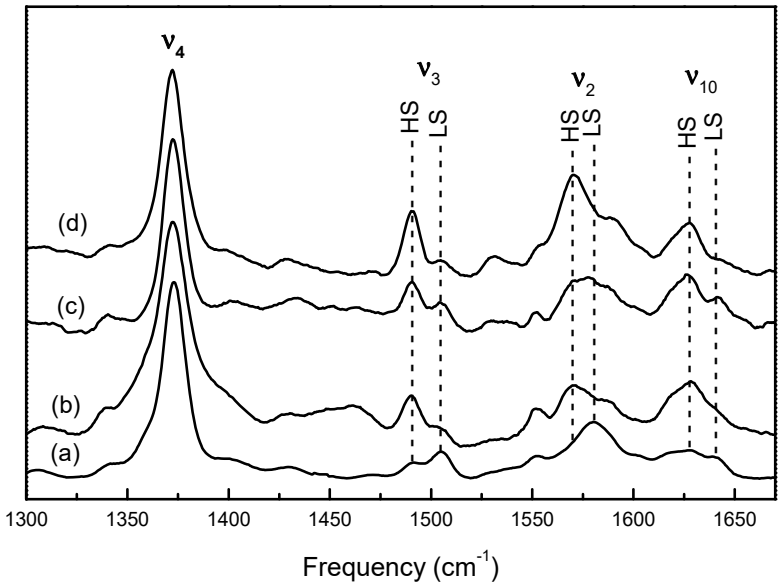


***Figure S6.*** High-frequency region of RR spectra of Aβ40-Fe(III)PP complexes**.** (a) pH 6.7; (b) pH 6.7 + 1 eq Cu(II); (c) pH 9.0; (d) pH 9.0 + 1 eq Cu(II). Excitation : 413.1 nm